DEVELOPMENT OF A SYNTHETIC QUARTZ DOSIMETER

DEVELOPMENT OF A DUAL PURPOSE SYNTHETIC QUARTZ OSCILLATOR/EMERGENCY DOSIMETER

by

Jonathan J. Liberda B.Sc.

A thesis
Submitted to the School of Graduate Studies
in partial fulfillment of the requirements
for the degree of
Master of Science

McMaster University

MASTER OF SCIENCE (2008) McMaster University

(Earth Sciences) Hamilton, Ontario

TITLE: Development of a dual purpose synthetic quartz oscillator/emergency dosimeter

AUTHOR: Jonathan J. Liberda, B.Sc. (McMaster University)

SUPERVISORS: Drs. W. Jack Rink and Douglas R. Boreham

NUMBER OF PAGES: xii, 85

Abstract

In the event of large scale public radiation exposures, a means of rapid personal radiation dosimetry would provide a valuable tool for environmental and human health protection as well as for possible criminal investigations (in the event of terrorist dirty bombs). This thesis describes a method of sensitizing synthetic quartz oscillators, found in many timekeeping devices such as watches and cellular phones, to function as radiation dosimeters.

Experiments on the sensitization of synthetic quartz crystals from watch oscillators were performed by subjecting the quartz to thermal treatments in the range of 200°C to 800°C. The lengths of treatments ranged from numerous one hour cycles to week-long single anneal treatments and combinations of the two. All treatments were designed to mimic factors that are known to cause sensitization in geologic quartz grains (Bøtter-Jensen, Larsen et al., 1995).

The greatest sensitization was observed in crystals treated to 800°C for one week and then subjected to two series of heating, irradiation, and optical exposures. These crystals were able to recover doses as low as 0.5 Gray at an error within 10% of the delivered dose. This work is the first stage of development for creating dual purpose quartz oscillator-dosimeters which could be used in watches, cellular phones, clocks, and nearly all equipment requiring a timekeeping component. In the future, experiments should be conducted to show definitively that crystals still function as 32.768 kHz oscillators after annealing and that oscillators trap charge while in operation.

Acknowledgements

This thesis was possible through the support of numerous individuals who trained, taught, and guided me throughout my academic career. In particular I am grateful to Dr. Douglas Boreham who took a chance by hiring an Earth Sciences student to perform radiobiological research, giving me a start in interdisciplinary science and thinking. Working in the company of Mrs. Nicole McFarlane, Mrs. Mary-Ellen Bahen, and Dr. Jennifer Lemon throughout the years has not only improved my research but made the laboratory a great place to work. I am also thankful to Dr. Jack Rink whose scientific intuition and broad knowledge have made me a better scientist and helped move my project through its most difficult problems.

I also appreciate the help I received throughout my thesis from my lab colleagues Kevin Burdette, Jeroen Thompson, Gloria López, April Stevens, and Chantel Iacoviello. Our discussions gave me a fresh perspective on problems I was facing and the good company was always appreciated. I would also like to mention Mr. Jim Garrett of the Brockhouse Institute for Materials Research who helped me a great deal in developing a method of graphite removal for the quartz crystals.

Lastly, I am appreciative of the academic environment in both the School of Geography and Earth Sciences and the Department of Medical Physics that enabled me to focus on questions relating to my research as opposed to discipline.

For my parents

Contents

List of Figures

List of Tables

List of Acronyms

SAR – Single Aliquot Regeneration Protocol

OSL – Optically Stimulated Luminescence

keV – Kiloelectron Volt

LED – Light emitting diode

EPR – Electron Paramagnetic Resonance

TL - Thermoluminescence

ED – Estimated Dose

Chapter 1
Introduction

1.1 Research context

The atomic age has given humanity new medicines, new technologies, and a new energy source. The cost has been large scale harmful radiation exposures to the public in both accidental and wartime scenarios. The Chernobyl disaster and the atomic bomb detonations over Hiroshima and Nagasaki are examples of the dangers now faced by humanity. However, these risks have been reduced through new reactor designs, security measures, and damage mitigation technologies. In the event of large scale radiation exposure from accidental or malicious radiological release, personal dose exposure assessment would provide a valuable tool for triage, future environmental and health risk, and criminal investigations.

There are two general categories under which personal emergency dosimetry methods fall. The first is biological dosimetry, which relies upon measuring a biological endpoint and correlating its magnitude to a radiation exposure. Examples of biological assays that can be used for dose determination are the micronucleus and fluorescent *in-situ* hybridization assays. Biological dosimetry has its advantages and drawbacks. The major advantage of biological dosimetry is that the dose measured was delivered directly to the tissue being examined and leaves relatively little uncertainty about the radiation dose to the rest of the body. These tissues, such as blood for cytogenetic assays, would also be readily available for analysis. A major drawback of biological dosimetry is that measurements and models often need to contend with large inter- and intra-individual

variability in regards to radiation exposure effects (Liberda, Schnarr et al., 2005). These variations make biological endpoints difficult to correlate to a radiation exposure since individual responses may vary from the mean. A second category under which emergency dosimetry methods fall is physical dosimetry. Physical dosimetry relies upon materials on or near the exposed person to determine a radiation dose. These materials can store charge released by ionizing radiation in a predictable way. Physical dosimetry does not require a standard curve for comparison since the aliquots themselves are used in dose regeneration. The major advantage of physical dosimetry is the sensitivity and accuracy of dose estimates, which can often resolve fractions of a Gray with a small error. Physical dosimetry methods also have the advantage of being equally sensitive to doses delivered in sequence, unlike biological dosimeters that often exhibit an adaptive response when irradiated. The largest disadvantage is the uncertainty in correlating this estimated dose to a biological exposure, as the sample being used in dose estimation may have been subjected to a different radiation field than the individual. Examples of physical dosimetry methods are optically stimulated luminescence (OSL) and thermoluminescence (TL). One particular method, electron paramagnetic resonance (EPR) lies between the biological and physical dosimetry categories. EPR requires the removal of biologically mineralized tissues such as teeth, however the dose measurements are performed on an inorganic mineral (Khan, Boreham et al., 2003). As such it is not a true biological dosimetric method despite the mineral source being biological in origin. This thesis is focused on the application of the physical dosimetry method OSL for use as an emergency dosimeter.

Optically stimulated luminescence (OSL) is commonly employed in the geological sciences to determine radiation dose exposures to quartz sediments. The dose obtained using OSL has been accumulated slowly over time due to constant irradiation from radionuclides in the soil and from the cosmic radiation flux. These doses can then be used to determine the time since burial once the total ***in-situ*** dose rate from all ionizing radiation sources is estimated (Huntley, Godfrey-Smith et al., 1985). The success of OSL in recovering radiation doses has also made it attractive as a means of retrospective dosimetry. Thomsen (2004) used OSL to determine the dose delivered to quartz grains in bricks to assess their suitability as dosimeters. While quartz in sediment and brick near the exposed individual may provide estimates of dose, the assumption that the individual received an exposure near the dose measured is difficult to prove and can be affected by anisotropic irradiation exposure as well as the distance of the individual from the sampling site. Fortunately, quartz crystals can be found around the wrist (watches) or in the pocket (cellular phones) of many individuals. These items are held in close proximity to the individual and would receive a dose very similar to that delivered to the tissues; a major advantage over using materials such as bricks. However, the quartz in watches and cellular phones do not have the radiation sensitivity and ideal behavior needed for accurate dose determination. Untreated synthetic quartz give luminescence signals barely distinguishable from background, making reliable dose estimation impossible for these samples (Rink, Pekar, & Boreham. Personal communication, 2006).

This thesis will illustrate how synthetic quartz intended for use as an oscillator in a wristwatch can be sensitized to radiation in order to overcome this obstacle.

Sensitization experiments performed on the synthetic quartz oscillators will be assessed. These experiments were performed using two general procedures. One means of sensitization was to mimic the heating and cooling cycles of the OSL single aliquot regeneration protocol, where crystals are known to be sensitized during the preheat, irradiation, and heating luminescence procedure (Banerjee, 2001). The second means of sensitization was to anneal the crystals for one week at elevated temperatures. Previous experiments investigating sensitization have found that anneals, even during preheat treatment, have a strong effect on the stimulated luminescence signal (Jungner and Bøtter-Jensen, 1994; Bøtter-Jensen, Larsen et al., 1995). Ultimately a combination of high temperature one week annealing, plus additional heating, irradiation, and light exposure cycles (structured as a SAR protocol) were able to sensitize the crystals so that they could be reliable emergency dosimeters, recovering doses as low as 0.5 Gray with a maximum of 10% error from the delivered dose.

1.2 Focus of Research

The goal of this research is to determine a method of sensitizing quartz crystal oscillators to radiation so that they are sensitive enough to reliably resolve biologically-relevant radiation doses as low as 0.5 Gray. In order to accomplish this, research into the treatments known to sensitize quartz to radiation were explored. In particular, heat treatments were used to sensitize the crystals. The heat treatments involved long term anneals in the temperature range of 200°C to 800°C, as well as heat cycling.

1.3 Importance of research

Practically, this thesis will be useful as a means of optimizing the sensitization of quartz watch crystal oscillators to radiation. By sensitizing the crystals, they may serve as emergency radiation dosimeters as well as fulfill their original function as oscillators. Thus, if an individual were irradiated, their watch could be disassembled, the quartz crystal removed, and the radiation dose determined using OSL.

This research will also provide insight into the processes that result in sensitivity change in quartz. The sensitivity change of quartz during OSL measurement has been widely observed (Bøtter-Jensen, Larsen et al., 1995; Nakagawa and Hashimoto, 2003). This sensitivity change had been problematic for geological dose determination using OSL since repeated measurements are desired in the OSL protocol. To account for sensitivity change Murray and Wintle (2000) introduced the SAR – single aliquot regeneration protocol which corrects for sensitivity change by using a test dose (SAR will be explained in greater detail later in this thesis). This test dose standardizes the changing sensitivity of the sample response to radiation. Furthermore sensitivity increases in the crystal, observed as an increase in the signal of the constant dose, provides a measure of sensitivity change. This correction, while valuable for the dose estimation process, does not account for the processes and mechanisms underlying the change in sensitivity. Moreover, the sensitivity change process is only partially explained using the current three trap and two recombination centre OSL model explained later in this work. This thesis closely examines the sensitization of synthetic quartz at relatively low temperatures

and through numerous heat cycles. These lower temperature treatments and cycles help elucidate some aspects of quartz sensitization to radiation.

Chapter 2
Literature Review

2.1 Current model of luminescence

OSL relates stimulated luminescence to a prior radiation dose delivered to the crystal. Figure 1 presents a schematic of the OSL process from the perspective of electron energy transitions. Ionizing radiation excites electrons from the valence to the conduction band (far left). These electrons are now "free" and have enough kinetic energy to be able to move about in the crystal lattice. The electrons can then relax into electron traps, such as the shallow, OSL, and deep traps shown. Traps are defects in the crystal lattice which are formed from vacancies, deformed lattice sites with more than the expected number of atoms, from the presence of atoms with a different number of valence electrons than silicon or, as is the case for germanium, differences in electronegativity and electron affinity (Ikeya, 1993). These traps create energy levels in the forbidden region between the valence and conduction band of the quartz crystals. This allows electrons to become trapped at a higher energy level than they would normally be allowed to occupy. The shallow traps have a relatively small energy difference between the electron state and the conduction band. This means that these electrons can be excited back into the conduction band at temperatures of 125°C and are slowly emptied even at room temperature, making them impractical for geological dating applications. The deep traps contain electrons that cannot be excited without high temperature anneals. The large amount of energy required to excite these electrons makes them impractical for dose estimation. The intermediate energy level labeled "OSL" has the ideal properties of being thermally stable for long periods of time and electrons in this trap can be stimulated using light in the visible

spectrum. Shining blue light on the crystals re-excites the electrons out of the "OSL" traps and back into the conduction band where they can once again relax to a lower energy state. A proportion of these relaxing electrons will fall into a luminescent recombination centre (shown towards the right of Figure 1), releasing the excess energy as ultraviolet radiation. Non-luminescent recombination centers also compete for relaxing electrons but do not emit light in the ultraviolet range. Instead they release the energy difference from the trap to the conduction band through bond vibrations (Pacchioni, Ieranò et al., 1998). Recombination centers (also called holes) are relatively stable locations of positive charge which were often formed by the ionization of the crystal during irradiation. Holes are created when electrons are excited to the conduction band leaving behind a positively charged ion. Electrons from elsewhere in the crystal that move to this positive charge leave behind a positive ion themselves, thus causing hole migration through the crystal though not resulting in the elimination of an unbalanced charge. The migration of holes takes place much more slowly than the migration of free electrons through the crystal lattice. Hole migration should not be confused with recombination, which involves the elimination of unbalanced charge at the defect site.

Figure 1: Energy level diagram of traps and recombination centers

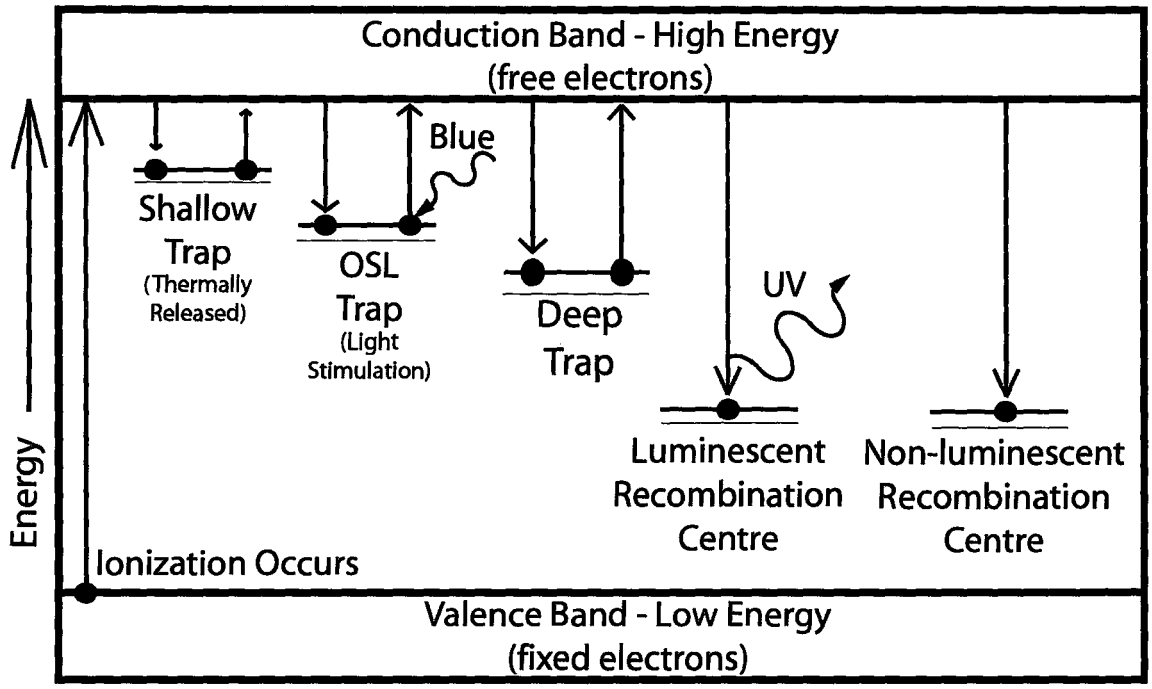

The exact nature and underlying mechanism of trap and hole formation which makes OSL possible rests largely upon the chemistry of titanium and aluminum. It has been observed using EPR that upon optical stimulation (after a high temperature anneal to remove the *E'* centers) equal numbers of $[AlO_4]^0$ holes and $[TiO_4/Li^+]^0$ / $[TiO_4/H^+]^0$ traps are removed, strongly supporting the hypothesis that recombination occurs though the elimination of these particular defect sites, with only a limited contribution of other defect sites (Poolton, Smith et al., 2000). From EPR studies it is known that $[AlO_4]$ acts as a hole trapping centre (Ikeya, 1993). This arises due to the charge imbalance caused by having an aluminum atom surrounded by four oxygen atoms in the quartz lattice. Aluminum has the ground state electron structure of *[*Ne*]* $3s^2\ 3p^1$ which enables the three valence electrons to bond only with three oxygen atoms as opposed to the four bonds formed by silicon whose electron configuration is *[*Ne*]* $3s^2\ 3p^2$. The lack of four valence

electrons results in an additional negative charge at the defect site $[AlO_4]^-$ caused by having an additional unbounded oxygen atom. This extra electron is more easily removed from the $[AlO_4]^-$ defect site than the quartz SiO_4 bond, thereby enabling the aluminum defect site to preferentially lose its electron, forming a hole trapping centre $[AlO_4]^0$. Electrons that recombine at these hole sites during stimulation often have their origin in titanium based impurities such as $[TiO_4/Li^+]^0$ and $[TiO_4/H^+]^0$ (Schilles, Poolton et al., 2001). Titanium's electron shell configuration is [Ar] $3d^2$ $4s^2$ which would enable the four electrons in the 3d and 4s orbitals to form covalent bonds with oxygen, the same number of bonds as silicon. However, since oxygen has a higher electronegativity of 3.5 than titanium at 1.5 , the four bound oxygen atoms pull the electrons in the covalent bond away from the titanium atom and leave the titanium nucleus relatively unshielded (Chang, 1998). The weakly shielded titanium atom is then capable of trapping a free electron from the conduction band, similar to the electron trapping process thought to occur in the germanium defect (Ikeya, 1993). The $[TiO_4 \bullet e^-]$ is then stabilized by a small and mobile cation such as Li^+ or H^+, thereby forming $[TiO_4/Li^+]^0$ or $[TiO_4/H^+]^0$ defect sites in the crystal lattice (Ikeya, 1993). Most importantly, titanium also functions well as an electron donor during light stimulation because of its extremely low 8 kJ/mole electron affinity which, compared to the 134 kJ/mole electron affinity of silicon, makes Ti an ideal electron donor since ionization occurs relatively easily (Chang, 1998).

2.2 Luminescence sensitivity change

Dose sensitivity is the amount of detected luminescence per dose unit delivered. Luminescence sensitivity change refers to the increase or decrease in stimulated signal

measured after equal radiation doses given to the same sample. Sensitivity change in a sample creates the problem of having equal doses in the same aliquot recover different signal magnitudes. Then, when the dose of interest is being recovered, the signal measured may not be a stable measure of the dose delivered. OSL sensitivity change has been widely observed in geologic quartz and has been studied in the OSL forerunner dosimetry method, thermoluminescence (TL). TL and OSL arise from the same electron traps in the quartz crystal, the difference being that TL uses heat to excite the electrons to the conduction band and OSL uses light to excite these same traps (Aitken, 1998). The sensitivity change of thermoluminescence (TL) due to heating and irradiation has been recognized since the methods early inception (Zimmerman, 1971). Because OSL and TL rely upon stimulating the same electron traps for dose determination, OSL sensitivity change was also observed (Bøtter-Jensen, Jungner et al., 1993; Bøtter-Jensen, Larsen et al., 1995). In order to improve the accuracy of dose estimation the sensitivity change of quartz has been subject to much experimentation, with natural and synthetic samples being investigated at a variety of anneal temperatures (Schilles, Poolton et al., 2001; Kale and Gandhi, 2008).

OSL sensitivity change from room temperature to 1000°C was studied in depth by Bøtter-Jensen, Larsen et al, (1995) who annealed natural and synthetic quartz and measured the sensitivity enhancement. They found little sensitivity enhancement from room temperature to 500°C, and observed a rapid rise in sensitivity from 500°C to 800°C. Annealing above 800°C led to a reduction in sensitivity. This paper also modeled how an increase in luminescent recombination centers and a decrease in non-luminescent

recombination centers affected OSL sensitivity. The model used three trap centers: one shallow, one deep, and one stimulated by blue light, and two recombination centers, one being luminescent and the other being non-luminescent. They were successfully able to model OSL supralinearity at lower doses and reproduced the enhanced OSL sensitivity for the annealed cases.

Another successful model was developed by McKeever et al. (1997) based upon the interacting three trap and two recombination centre system proposed by Bøtter-Jensen et al. (1995). In this case, computer simulations were used to examine the role of shallow and deep traps as related to sensitization during the OSL procedure. Their model suggests that the shallow traps are responsible for the initial major change in sensitivity and that the presence of shallow and deep trap interactions prevents a sensitivity decrease. The authors also suggest that shallow traps affect sensitivity change in the crystal through two possible effects. The first effect is recuperation, where a portion of the charge excited from the OSL trap during blue light stimulation relaxes into shallow traps. When the sample is pre-heated some of the charge in the shallow traps is again trapped in the OSL trap, causing charge to accumulate from the former and latter irradiations. The second effect is competition, which claims that natural irradiations occur over time periods much greater than the lifetime of residence in the shallow traps. However, laboratory irradiations occur in much shorter periods of time when the effect of the shallow trap is not negligible and there may be charge remaining in the shallow traps. There may also be differences in trapping dynamics between OSL stimulations. To account for both these

scenarios the authors suggest that OSL measurement and irradiations should be undertaken at elevated temperatures.

While the effects of shallow and deep traps can explain some aspects of sensitivity change in a broad way, there have also been studies to identify how specific defects are affected by annealing. The *E'* center in silica is formed by a positively charged hole trapped at an oxygen vacancy, its structure is $(\text{-O})_3\text{Si}\bullet + \text{Si}(\text{O-})_3$ and it has been shown to act as a non-luminescent recombination centre (Pacchioni, Ieranò et al., 1998). The *E'* centre can be observed in quartz using EPR. The *E'* centre has been shown to be annealed out at temperatures ranging from 300° to 870°C depending on the type of quartz and whether any etching was undertaken (Poolton, Smith et al., 2000). Therefore, when annealing quartz at high temperature some of the increase in sensitivity is due to the removal of these non-luminescent recombination centers.

The presence of impurities is also known to influence the luminescence signal of quartz, though their concentrations will remain stable in the crystals throughout the SAR protocol (Hashimoto, Sakaue et al., 1994). It is likely that impurities affect sensitivity if they are re-distributed throughout the crystal when subjected to anneals (Poolton, Smith et al., 2000). For example, at anneals beyond 870°C it is believed that $[TiO_4/H^+]^0$ centers become unstable and dissociate, allowing $[TiO_4/Li^+]^0$ centers to form from the available Ti atoms (Poolton, Smith et al., 2000). This results in a decrease of the crystal sensitivity.

Chapter 3
Methods

3.1 Overview of methods

Oscillator cylinders containing the quartz crystals were purchased from Digikey, an electronics supplier. While all the cylinders ordered were the same model, it is possible that the crystals themselves may have been formed from various lots of synthetic quartz. All oscillators were "AT" cut from the main synthetic crystal. AT is the cut for timekeeping oscillators that operate at the standard frequency of 32.768 kHz. To obtain the quartz crystal the casing and graphite covering was removed; both processes are explained in detail in later sections. Once the crystals were cleaned they were subjected to the treatment of interest: heating or light exposure. For heat treatments, a furnace was preheated to the appropriate temperature and crystals were placed into the furnace in fused silica crucibles. Temperature was monitored using the furnace temperature gauge and verified with a thermocouple. Irradiations were completed in the Risø automated TL/OSL reader (Risø, Roskilde, Denmark) using the integrated $^{90}Sr/^{90}Y$ beta source. Experiments involving light exposure used a halogen lamp with a broad light spectrum that mimics the sun's rays. Light exposures were completed by placing crystals in a single layer on a Pyrex glass dish, the dish was then placed under the light for the time period desired.

3.2 Casing Removal

Commercial quartz oscillators were encased in metal (Figure 2) and ready to be soldered into a watch. All experiments were carried out with crystals contained in model number

"CFS206-32.768KDZB-UB" by manufacturer "Citizen" ordered through Digikey. Since the quartz crystal itself was required for dosimetry it was necessary to remove the metal casing. The casing metal was oxidized using a bath of aqua regia, consisting of: 25% (vol) 16 M nitric acid and 75% (vol) 16 M hydrochloric acid. The hydrochloric acid and nitric acid were added in excess (total of 40 mL) to groups of 20-30 casings in 50 mL plastic centrifuge tubes. The addition of excess acid ensured that the heat produced during metal dissolution did not affect the crystal properties. Once the solution ceased bubbling, the acid was aspirated using a pipette. The crystals were then collected and rinsed thoroughly using deionized water.

Figure 2: Crystals contained in the metal cylinder

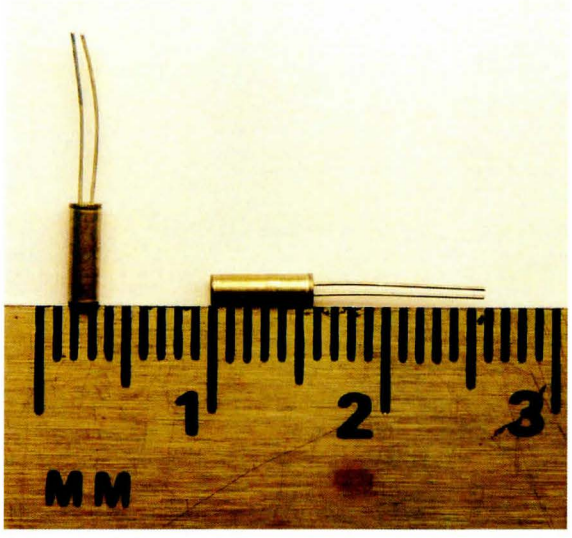

3.3 *Graphite Removal*

Figure 3 shows the dark covering on the quartz crystal oscillators which acts as an electrical contact for crystal oscillation. This covering would interfere with the measurement of luminescence meaning that removal was necessary before annealing experiments began. It was first essential to determine the composition of the coating. To accomplish this, energy dispersive spectroscopy was performed, the results of which are shown in Figure 4. The small peak around the energy 0.25 keV, labeled "C", positively identifies the coating as carbon. Initial attempts to remove the coating through physical abrasion were of limited success. The most successful attempt at removal of the carbon coating using physical abrasion involve placing 1 mm diameter grains of silica carbide into a tumbler with 50 crystals. The tumbler was then operated until the softer graphite was removed, usually requiring many weeks of tumbler operation. Unfortunately, parts of the graphite coating were often left on the crystal, particularly near the tip of the forks, and so this method of graphite removal was abandoned. An alternative chemical means of graphite removal was used in all crystals examined here. To remove the graphite, a saturated solution of fresh sodium hydroxide was prepared and groups of 50-150 crystals were sealed into 2 mL plastic tubes with this basic solution. The tubes were then placed into an oven at 80°C for 4 weeks, after which all the graphite was dissolved. It may be possible to achieve faster graphite dissolution if the temperature of the sodium hydroxide treatment is increased beyond 80°C. After treatment the crystals were rinsed thoroughly using deionized water and any crystals with quantities of graphite still attached were rejected. The bare crystals which resulted from this treatment are shown in Figure 5. The

dimensions of these crystals were measured using a micrometer. For a sample size of 10 crystals measured once, the average length of the crystals was 4.449 mm (taken as the distance from the tip of the split forks to the bottom of the attached base). For a sample size of 10 crystals measured twice, the average width of the crystals was 1.006 mm (measured across the base of the fork, from left to right in Figure 3). The thickness of 10 crystals, measured ten times at various points on the tuning fork and its base, was determined to be 0.232 mm. A sample of 35 crystals was weighed to 82.4 mg, giving an average weight of 2.4 mg per crystal.

Figure 3: Scanning electron microscope image of the quartz crystal oscillator

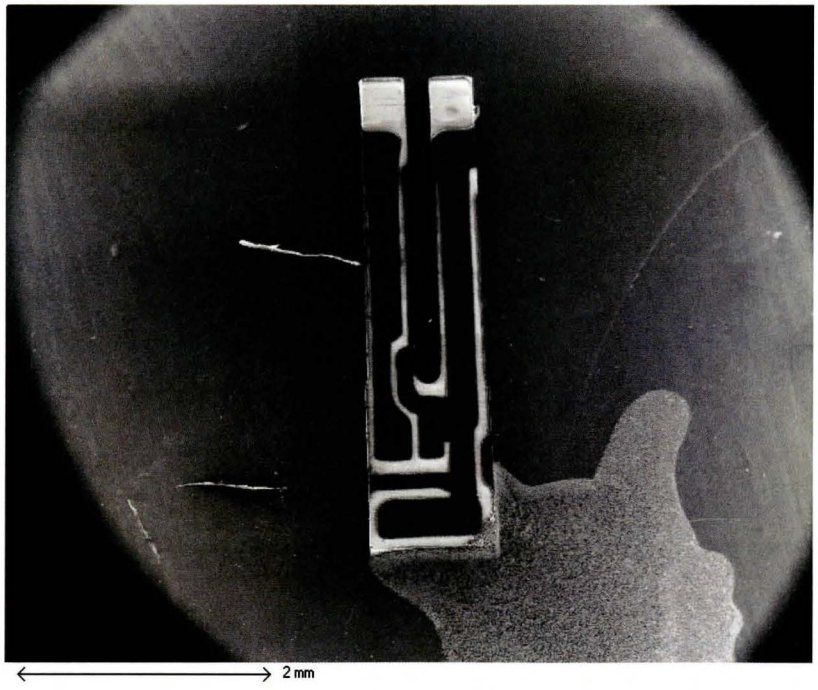

Figure 4: Energy dispersive spectroscopy confirming carbon composition of coating

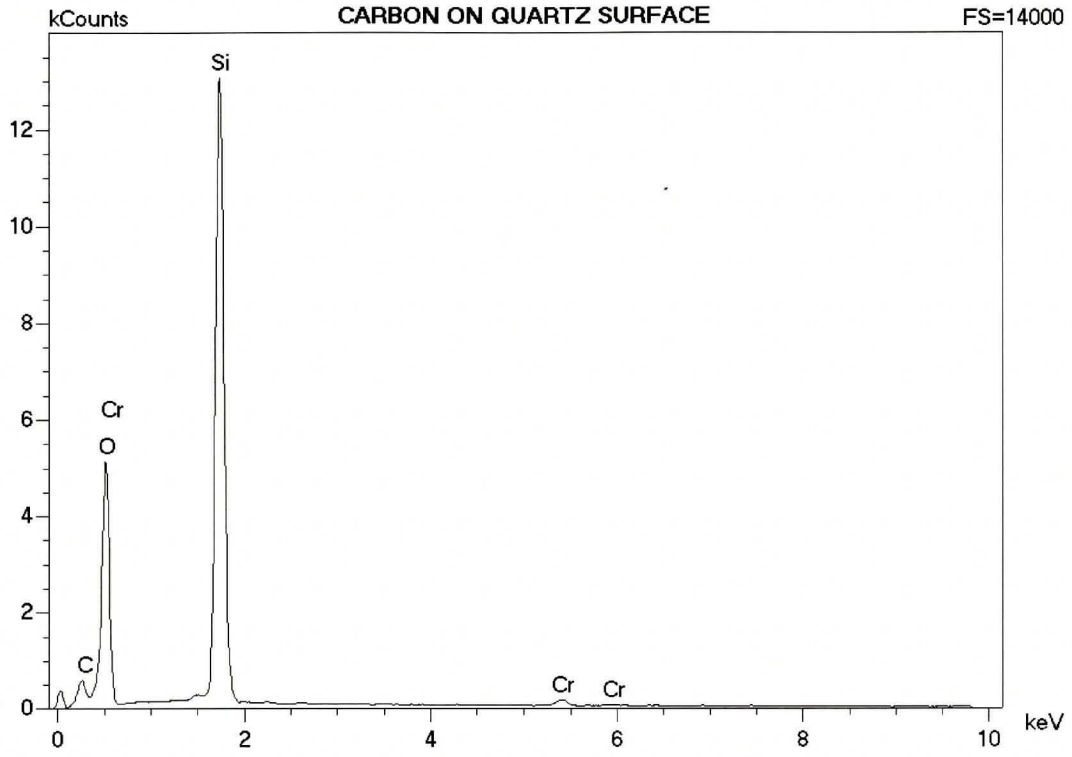

Figure 5: Crystals with the casing and graphite layer removed.

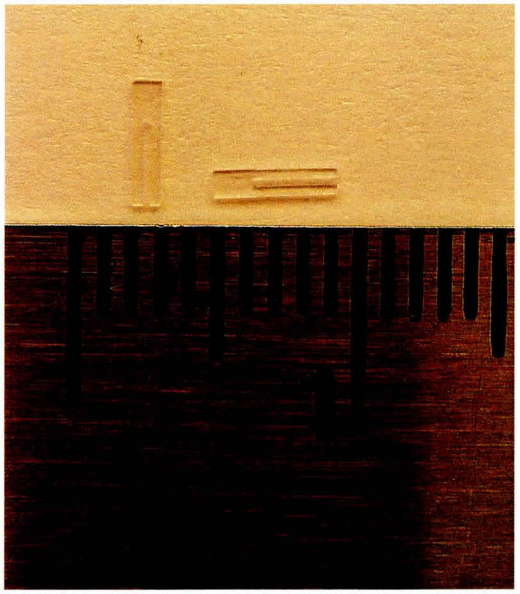

3.4 Risø automated OSL reader

Radiation doses absorbed by the quartz crystals were determined with a Risø automated OSL reader. The model used in this study was a TL/OSL System TL-DA-15. The OSL system used has two filters, both Hoya U-340, one 7.5 mm thick and the other 5 mm thick. Stimulation was provided by blue light emitting diodes operating at 470 nm. Figure 6 presents a schematic of the Risø automated OSL reader, though more detailed descriptions of the system are available from Markey, Bøtter-Jensen et al (1997). In order to prepare the sample for analysis by the Risø system, crystals were attached to aluminum disks for OSL measurement. Aluminum disks were first sprayed with silicone oil (silkospray). The crystals were subsequently mounted on the centre of the disks using tweezers as shown in Figure 7. After the crystals were attached to the disks they were loaded, a maximum of 48 disks at a time, into the Risø carrousel for analysis. The carrousel was then placed into the Risø reader where the Minisys computer followed the irradiation, heating, and light emitting diode (LED) stimulation sequence outlined by the user. The results of the experiments were recorded on a computer for analysis using the Risø analyst software program.

Figure 6: Schematic diagram of Risø automated OSL/TL reader (Thomsen, 2004)

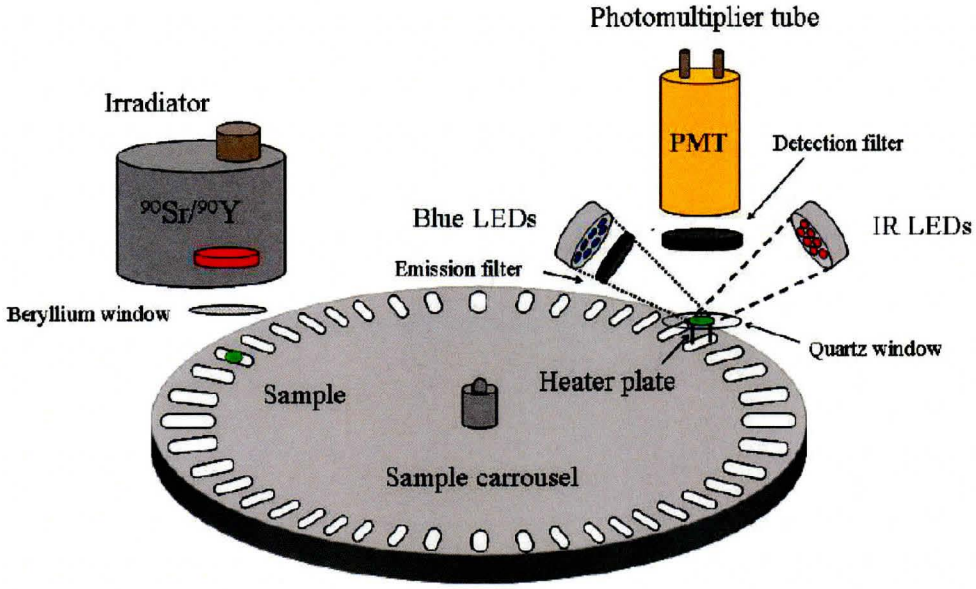

The effect of cross-talk to adjacent samples during irradiation is negligible. Cross-talk has been reported to be a maximum of 0.17% of the given dose to coarse quartz grains (Bøtter-Jensen, Bulur et al., 2000) and 0.04% to α-Al_2O_3:C dosimeters (Kalchgruber, Göksu et al., 2002). These errors are much smaller than the uncertainty of the doses measured in all cases here. Further, since all doses, including the regeneration dose, were given using the built-in beta source, the additional dose exposure to adjacent crystals caused by cross-talk would also occur for regeneration irradiations. The proportion of cross talk would remain the same for all doses delivered to the crystals and would effectively negate the effect of having a slightly increased radiation exposure to the samples.

The spatial variation in dose rate also merits some discussion. Since the sample crystals are not circular, as most grained aliquots are when placed onto the Risø disks,

there was a large amount of space left without any crystal cover. A picture of the aluminum disk with a mounted quartz oscillator is shown in Figure 7. Since the dose rate delivered to the disk has been shown to vary radially, in the order of 11%, the crystals were all mounted in the very centre of the disks (Veronese, Schved et al., 2007). This also follows the recommended means of mitigating the non-uniform dose rate by Ballarini, Wintle et al (2006). No other methods were used to correct for variation in delivered dose.

Figure 7: Crystal mounted on aluminum disk ready for analysis using the Risø

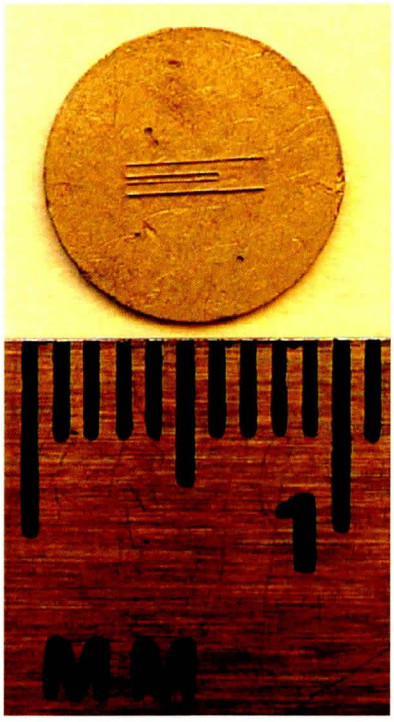

The photon count versus time graph, called a shinedown curve, shows the number of UV counts measured during blue light stimulation. The resulting plot roughly approximates a decaying exponential curve, as shown in Figure 8. The plot shown is a

shinedown curve measured from the synthetic quartz used in this work. There are in fact numerous overlapping exponential functions represented in a shinedown curve. These functions have their origin in fast, medium, and slow exponential decay components of the OSL process (Aitken, 1998).

The fact that there are many contributors to the shinedown curve means that the integrated signal used to determine the stimulated luminescence response can have a significant effect upon the dose estimate. This is particularly true since annealing has been shown to affect luminescence lifetimes and the proportion of fast, slow, and medium decay components presented in the shinedown curve (Chithambo, 2004). In this work only the first two channels, representing the first 0.8 seconds of luminescence stimulation, were integrated and used as the OSL signal for a given dose. These two channels would have the highest signal magnitudes of the entire shinedown curve and the greatest proportion of fast component in relation to medium and slow components. This is advantageous because the fast component would be almost entirely bleached over the 100 second stimulation time, while the slow component of the OSL signal may still retain some trapped charge that could be held until the next stimulation sequence. This is supported by findings that the slow component of the shinedown curve is most appropriate for Aeolian sediments, which would have been subjected to extensive bleaching before sedimentation (Singarayer, Bailey et al., 2000).

Figure 8: Typical shape of a shinedown curve observed using OSL

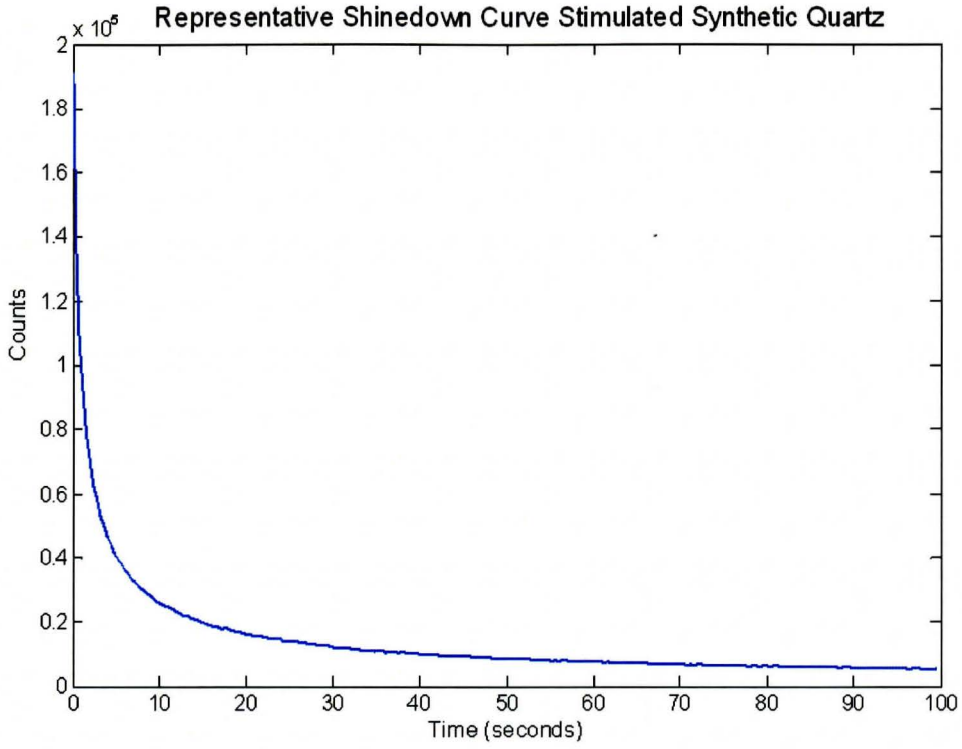

3.5 Data analysis for dose determination

The data obtained from the Minisys computer was analyzed using the Risø analyst software program (version 3.15b). An effort was made to accept as much data from all treatments as possible. Therefore, all error triggers were turned off: all recycling ratios were deemed acceptable, all test dose errors were deemed acceptable, and systematic error was increased up to 10% if necessary to fit an exponential equation to the regeneration data. The only case where data was not accepted for analysis was when the signals from a crystal could not be fitted with an exponential curve and could not provide an estimated dose. This was more prevalent for low sensitivity crystals, since the small signal for all doses delivered could not be well determined after the relatively high

background count was subtracted. The Risø software also provided an error with the estimated dose calculation which was used in all plots. For signal magnitude plots, all signals from the irradiation of interest in the treatment group were averaged and the standard deviation calculated. For the signal magnitude plots in the later sections of this thesis two standard deviations are included as error bars.

3.6 Single-aliquot regenerative dose protocol

To determine the dose with which crystals were irradiated, the single-aliquot regenerative dose protocol was used (Murray and Roberts, 1998; Murray and Wintle, 2000). This protocol relies on the use of a test dose to account for sensitivity change of the quartz throughout repeated OSL measurements. Its general format (from Murray and Wintle, 2000) is presented in Table 1. The doses delivered for regeneration increased in a linear fashion, with doses bracketing the original delivered dose of interest, either 30 seconds or 6 seconds. In total there were five regeneration doses, plus a zero dose and one repeated dose. The repeated dose was needed to calculate a recycling ratio and was set as the second lowest regeneration dose delivered. Estimated doses and their errors were calculated using an exponential equation fitted to the data using Risø Analyst software version 3.15b as per the method outline in section 3.5.

***Table 1: Generalized single-aliquot regeneration sequence** (Murray and Wintle, 2000)*

Step	Treatment	Observed
1	Deliver dose, D_i	-
2	Preheat to 160°C for 10 seconds	-
3	LED stimulation for 100 seconds	L_i
4	Deliver test dose, D_t	-
5	Heat to 160°C	-
6	LED stimulation for 100 seconds at 125°C	T_i
7	Repeat step 1 with a new D_i	-

Chapter 4
Results

4.1 Beta irradiation uniformity

In all experiments performed, the doses given to the crystals were delivered by the $^{90}Sr/^{90}Y$ β radiation source incorporated into the Risø system. This includes the "natural" dose which was to be recovered using the SAR protocol. The mean energy of electrons emitted by the $^{90}Sr/^{90}Y$ β radiation source are 195.8 ± 0.8 / 933.7 ± 1.2 keV (Energy Sciences and Technology Department, 2008). The penetration depth of the β radiation into the crystal is uniform because all doses were delivered isotropically. Therefore, the effect of β particle attenuation upon dose estimation can be ignored. It should be noted that for watch crystals which would be irradiated anisotropically, such as in a dirty bomb, the Risø system would need to be calibrated to the 232 μm thickness of the synthetic quartz crystals, or a correction could be applied to the estimated dose.

The extent of β attenuation through an irradiated crystal is calculated below. As the degree of β particle attenuation in quartz is similar to that of aluminum, the aluminum attenuation factor was used for calculations (Aitken, 1998). The β particle absorption coefficients in aluminum were 20 cm^{-1} for ^{90}Sr and 0.3 cm^{-1} for ^{90}Y (Knoll, 2000). The absorber thickness was 0.0232 cm which is the thickness of the quartz crystal as measured using a micrometer. To estimate the proportion of counts absorbed by the material, the initial condition (counts without the absorber) used was 1 million counts. In this way the relative diminishment of β particles through the material could be determined. Calculation of the β particle absorption followed the equation and units

outlined in Haemers et al. (2007). Equation 1 shows that the ^{90}Y β particle counts are only diminished by 0.7% due the presence of the quartz crystal, making the radiation flux at both sides of the crystal nearly identical. Equation 2 shows that the ^{90}Sr β particle counts are diminished by 37% due to the crystal presence, indicating a significant absorption of the incident β radiation as it passes though the crystal. This supports the previous conclusion that non-uniformity of laboratory dose would need to be accounted for in recovering doses from an anisotropic radiation environment, though it is not a source of error in this work since all crystals were irradiated uniformly.

Equation 1: Absorption of ^{90}Y β radiation for 232 μm crystal thickness

$$\frac{I}{I_0} = e^{-nt}$$

$$I = I_0 e^{-nt}$$

$$I = 1{,}000{,}000 \cdot e^{-0.3 \cdot 0.0232}$$

$$I = 993{,}064$$

Equation 2: Absorption of ^{90}Sr β radiation for 232 μm crystal thickness

$$\frac{I}{I_0} = e^{-nt}$$

$$I = I_0 e^{-nt}$$

$$I = 1{,}000{,}000 \cdot e^{-20 \cdot 0.0232}$$

$$I = 628{,}763$$

Where:

I = Counts with crystal in place

I_0 = Counts without crystal absorption

n = β particle absorption coefficient (cm^{-1})

t = Absorber thickness (cm)

4.2 Pre-heat temperature determination

Data from the dose recovery test are shown in Table 2 (correct dose is 500 seconds). The pre-heat temperatures investigated were up to a maximum of 280°C, beyond which the pre-heat begins to induce a significant sensitivity change in the aliquots (Murray and Roberts, 1998). For the 160°C pre-heat the two crystals that gave a response were both correct within uncertainty. The 160°C pre-heat also had the lowest percentage error associated with it. The correct estimated dose results and relatively low error of the 160°C preheat make it the optimal pre-heat temperature and so it was used as the pre-heat temperature in all experiments.

Table 2: Dose recovery test results

Pre-Heat Temperature (°C)	Estimated Dose (seconds). Correct is 500 seconds			Average
	Disk 1	Disk 2	Disk 3	
160	499.29 ± 38.04	N/A	528.98 ± 32.89	514.13 ± 50.56
200	483.60 ± 38.45	463.49 ± 90.35	617.48 ± 42.44	521.53 ± 109.80
240	659.90 ± 142.92	512.74 ± 72.06	N/A	586.32 ± 151.38
280	652.71 ± 88.59	584.17 ± 86.75	N/A	618.44 ± 124.44

Crystals not providing results due to improper curve fitting were marked as N/A.

A preheat plateau test was performed, however, due to the low sensitivity of the crystals, the estimated doses and uncertainties were very large. As a result, the test could not discern a plateau, or even a difference in estimated dose for the pre-heat temperatures of 160°C, 200°C, 240°C, or 280°C. Lastly, a thermal transfer test was not performed since all irradiations were completed in the laboratory. Therefore, the preheat temperature effect on thermal transfer of charge would not affect the estimated dose as it does in the

case of geological quartz. The laboratory irradiated crystals used in this thesis would not have pre-depositional trapped charge that can be excited into OSL traps making a thermal transfer test unnecessary. For all OSL runs performed in this thesis, the 160°C preheat was used based on the results of the dose recovery test.

4.3 Untreated Crystals

The SAR protocol was performed on crystals which only had their graphite coating removed; they were not subjected to any other sensitization treatment. This is the control result whereby improvements in estimated dose and signal magnitudes could be discerned. Dose estimates for run 1 and run 2 are shown in Figure 9 and Figure 10 respectively. For the untreated crystals a total of 10 crystals were used in the experiments. Along the x-axis the number of crystals providing a dose estimate out of the 10 crystals is listed. For the first run 8/10 crystals provided an estimated dose while for the second run all crystals could be used for dose estimation. In both runs the error is considerable; the best crystals had errors around 10 seconds, which is 33% of the given dose. The large error associated with these crystals, even at high doses, would limit their usefulness as emergency dosimeters. These crystals also demonstrate that larger signal magnitudes provide better ED results. For example, in the second run crystal 4 provided an excellent result for the ED and also had the highest signal magnitude of all the crystals examined. Crystal 1 had the largest error in the first run and also the lowest signal magnitude. This highlights the importance of increasing stimulated counts, as this enables dose estimations to be calculated with greater accuracy and a lower fitting error in the ED. For all untreated crystals the 30 second irradiation equals 2.53 Gy.

Figure 9: Dose estimated for untreated crystals – Run 1

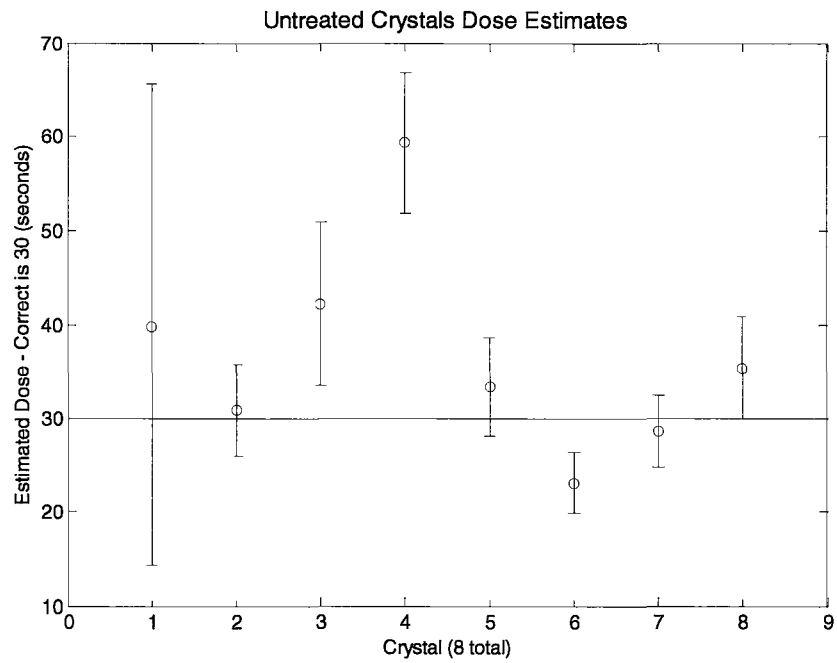

Figure 10: Dose estimates for untreated crystals – Run 2

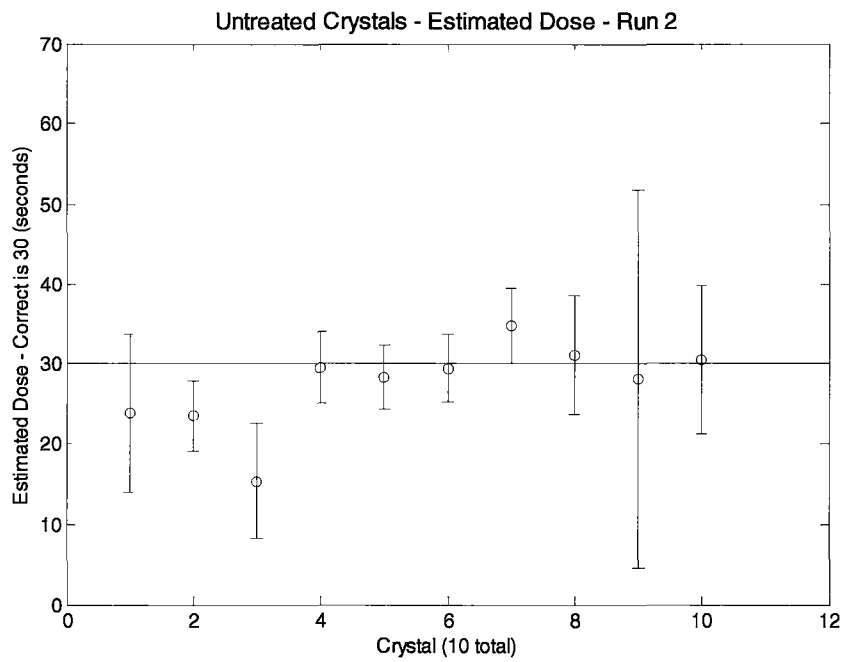

The signal magnitudes for the untreated crystals are low, with most crystals providing around 400 counts for the 30 second irradiation of the first run. For the second run the stimulated signal drops to around 300 counts for the same irradiation time. However, the decrease in sensitivity from the first to the second run is accompanied by an increase in the number of crystals providing data suitable for ED determination and most estimates were improved from the first to the second run. The accuracy of the ED results was also improved from the first to the second run, suggesting that some crystals provided better ED results for a lower signal magnitude. Despite this, for irradiations much shorter than 30 seconds, which is a dose of 2.53 Gy, larger signal magnitudes are needed since counts above background may be too small to distinguish.

Figure 11: Signal magnitude for untreated crystals – Run 1

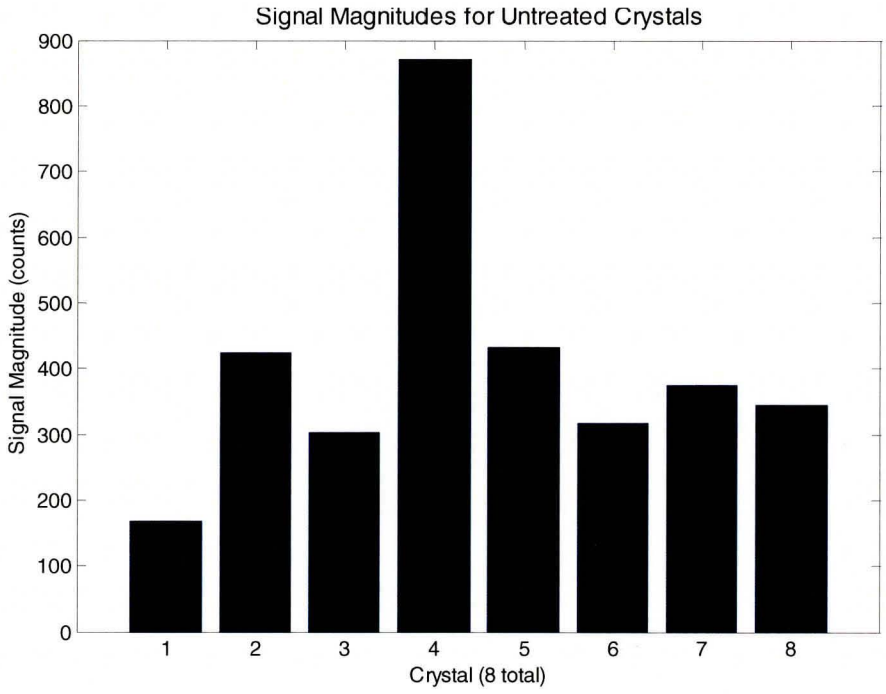

Figure 12: Signal magnitude for untreated crystals - Run 2

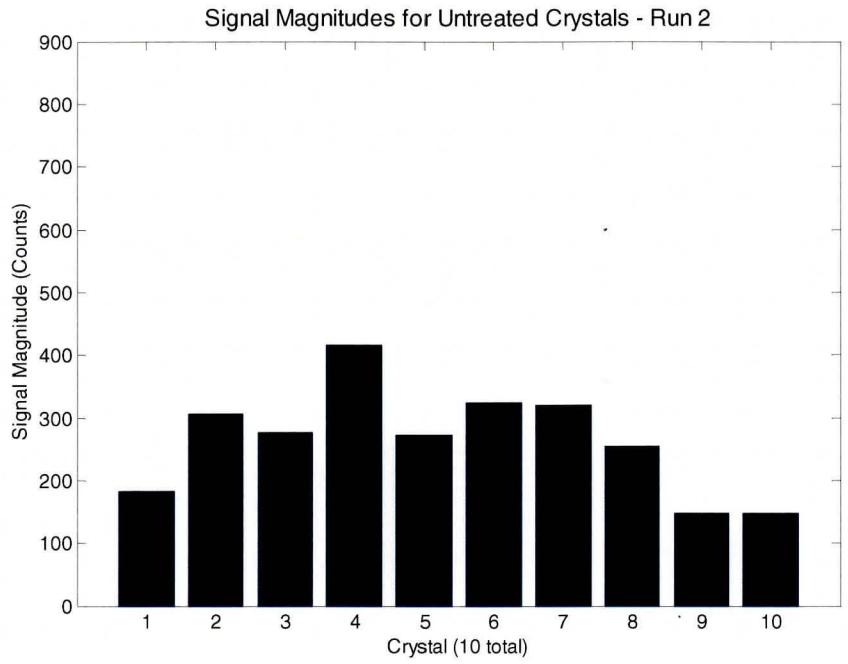

4.4 Solar Exposure Simulation

Light exposure experiments were meant to mimic the solar bleaching that occurs in sedimentary quartz of geological origin. These quartz grains, which are often used in OSL dating, are subjected to light exposures before burial; these exposures may play a role in the sensitization of the crystal. Bleaching also occurs during the SAR protocol during blue light stimulation, and the SAR protocol often causes sensitivity changes in the quartz being measured (Murray and Wintle, 2000). To determine the effect of light exposure upon radiation sensitivity, bare crystals were exposed to light from a halogen lamp for a period of four continuous days for a total of 96 hours. The halogen lamp emits a broad light spectrum ranging from the infra-red to the ultra-violet that approximates the wavelengths of light emitted by the sun. Figure 13 and Figure 14 present the results from

two OSL runs performed on these crystals after light exposures. For all bleached crystals the 30 second dose equals 2.53 Gy. For the bleached crystals a total of 10 crystals were used in the experiments. Along the x-axis, the number of crystals providing a dose estimate out of the 10 crystals treated is shown.

Figure 13: Dose estimates for bleached crystals – Run 1

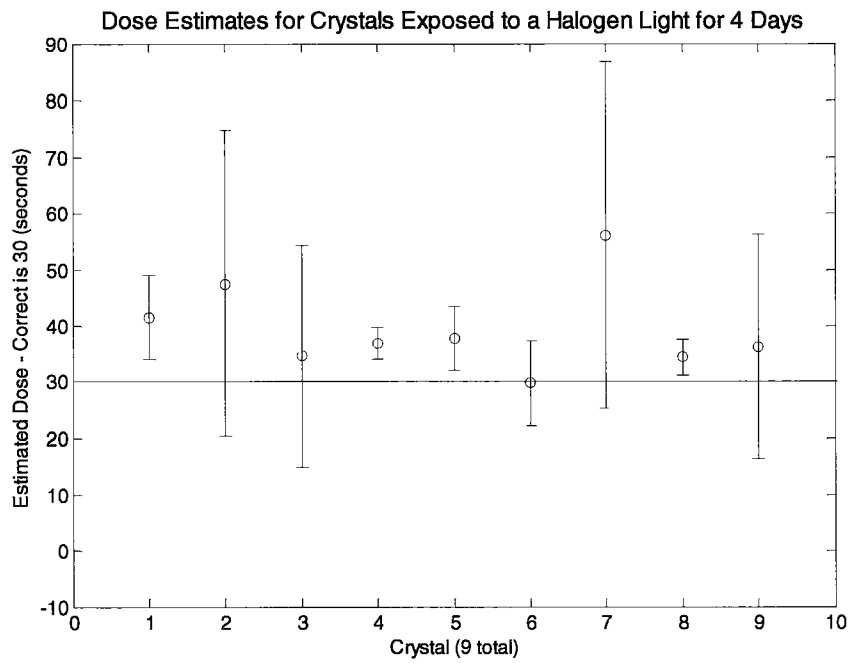

Figure 14: Dose estimates for bleached crystals - Run 2

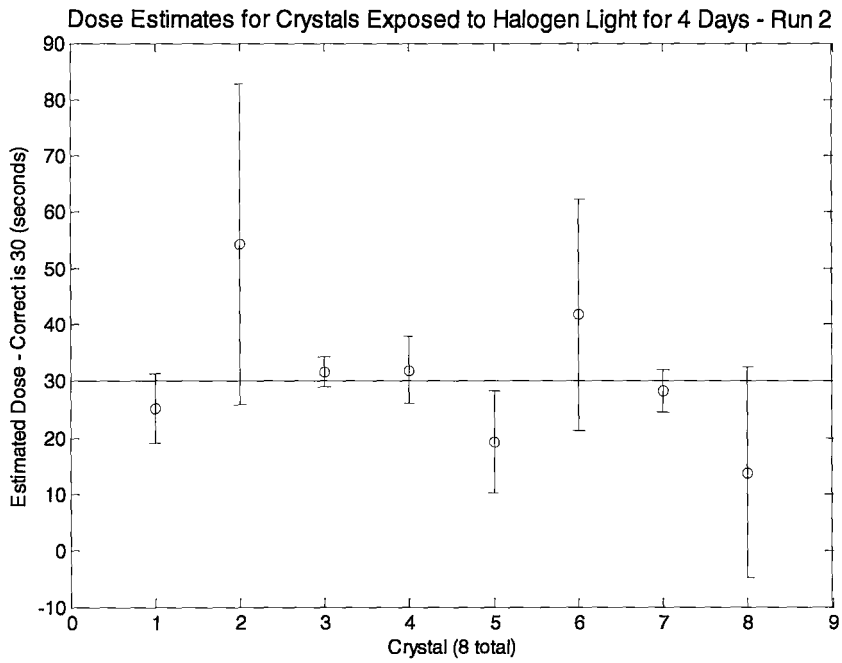

Signal magnitudes for run 1 and run 2 of the bleached crystals are presented in Figure 15 and Figure 16. The counts were very low for most of the crystals, with signals being around 150 counts. This is not an improvement over the 300 and 400 counts observed for the untreated crystals and seems to reflect a decrease in sensitivity after the long light exposure. As with previous observations, the crystals with the highest signal magnitudes, crystal 4 and 8 for run 1 and 3 and 7 for run 2, had the best ED results. As light exposure did not result in a major improvement of crystal sensitivity this treatment method was abandoned in favor of further annealing experiments.

Figure 15: Signal magnitudes for bleached crystals - Run 1

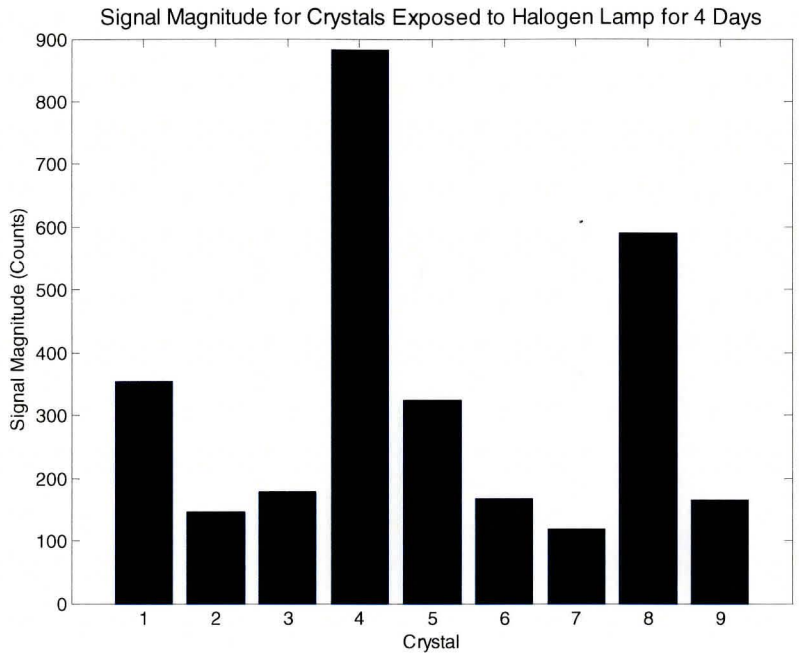

Figure 16: Signal magnitudes for bleached crystals – Run 2

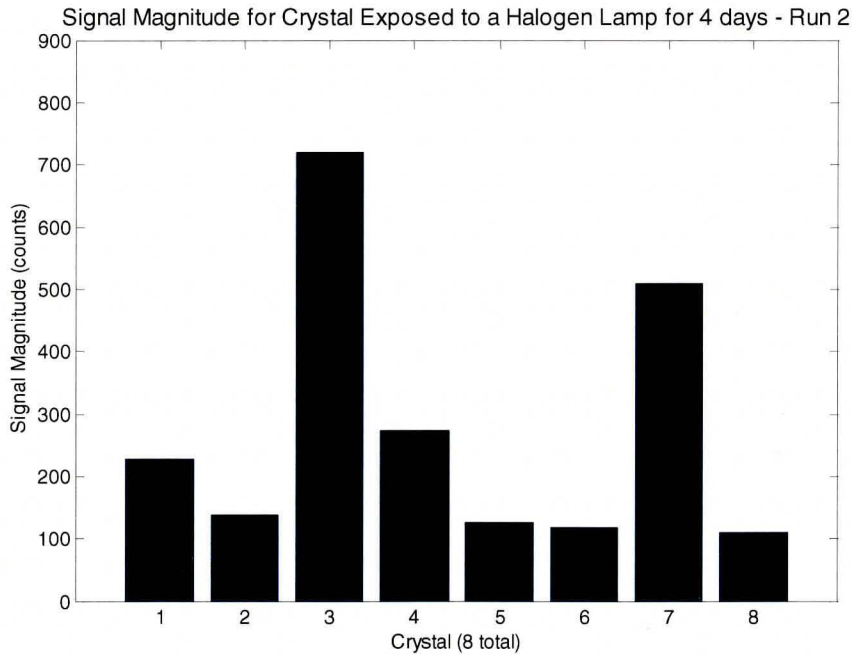

4.5 One week anneals

Annealing prior to irradiation has been shown to have a significant influence upon crystal sensitivity (Kale and Gandhi, 2008). A number of experiments were undertaken to take advantage of this phenomenon. The first of these involved annealing groups of 24 crystals for one week at the temperatures 200°C, 300°C, 400°C, or 500°C. All annealed groups were subject to two SAR runs since the crystals often continue to improve their ED results after an additional SAR treatment. The estimated dose results for both runs for all treatment temperatures are shown from Figure 17 to Figure 24. For the one week anneal experiment, groups of 24 crystals were used in each treatment. The x-axis shows the number of crystals providing dose estimates out of the 24 treated. Some crystals did not provide an ED, in these cases the regeneration dose data could not be fitted with a mathematical expression and the crystal data was rejected. Only in the 500°C treatment group did all 24 crystals provide an ED for both runs. For the 200°C treatment group, the first run had 24 crystals provide ED results and the second run had 22 crystals provide data. Despite these apparently good results for the 200°C treatment group, the error associated with the ED were large, often 50-66% of the delivered dose. The 500°C treatment group was much improved in this regard and had much lower ED error, often in the range of 17-33% of the delivered dose. This makes the 500°C annealed crystals much more appealing for dose estimation and so it was used as the initial annealing treatment for later heat cycling experiments. For all one week annealed crystals the 30 second irradiation equals a dose of 2.52 Gy.

Figure 17: Estimated Dose for Crystals Annealed for 1 Week at 200C – Run 1

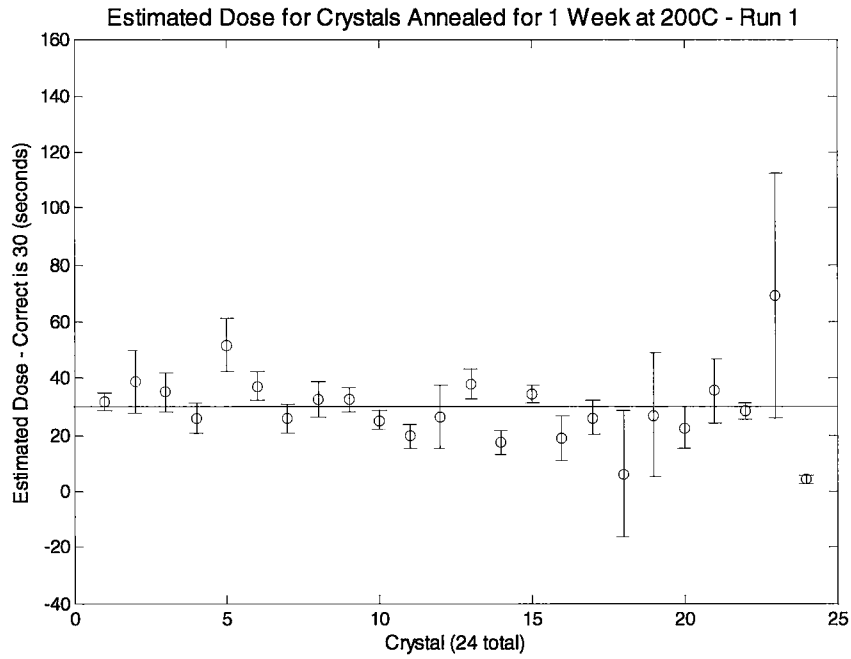

Figure 18: Estimated dose for crystals annealed for 1 week at 200°C – Run 2

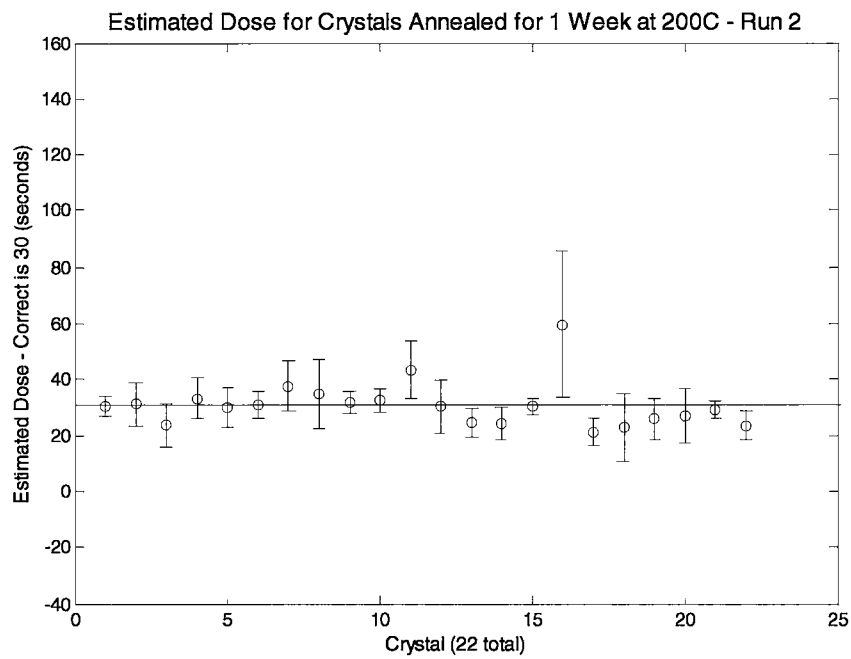

Figure 19: Estimated dose for crystals annealed for 1 week at 300°C – Run 1

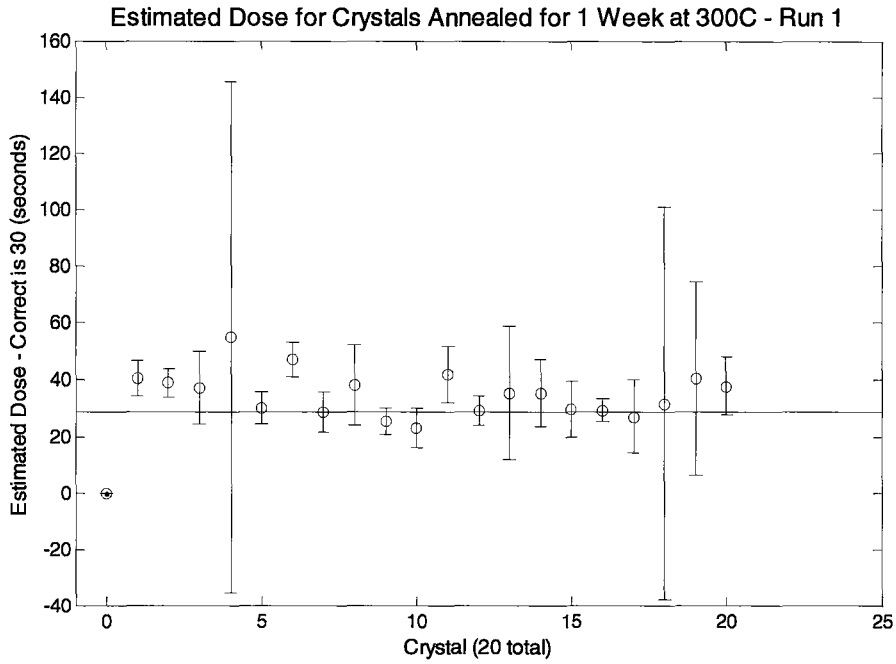

Figure 20: Estimated dose for crystals annealed for 1 week at 300°C – Run 2

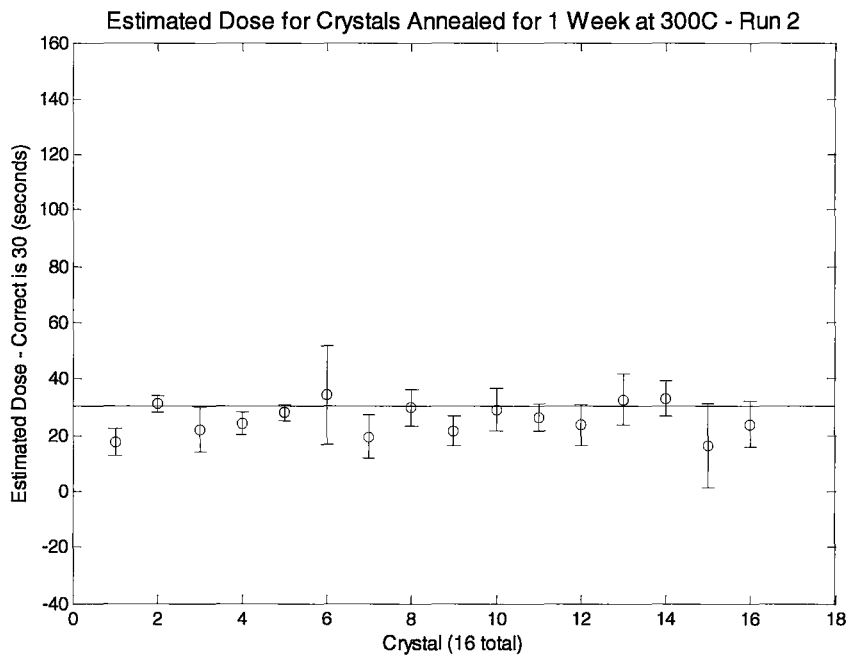

Figure 21: Estimated dose for crystals annealed for 1 week at 400°C – Run 1

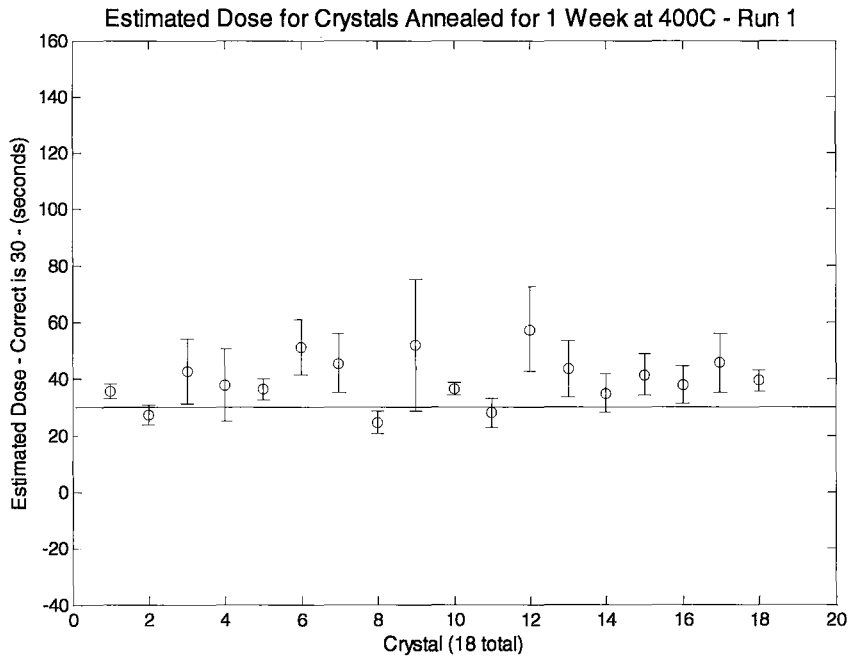

Figure 22: Estimated dose for crystals annealed for 1 week at 400°C – Run 2

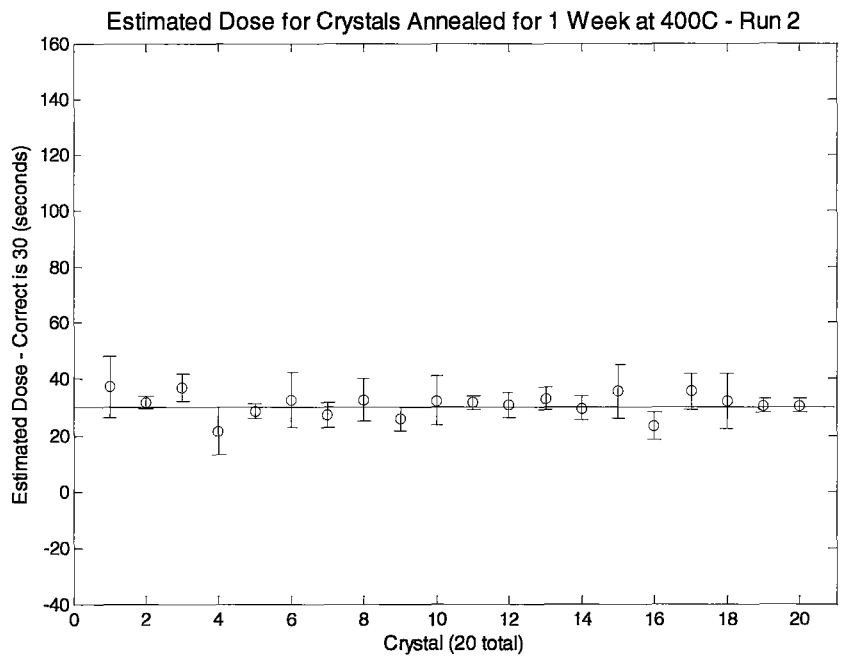

Figure 23: Estimated dose for crystals annealed for 1 week at 500°C – Run 1

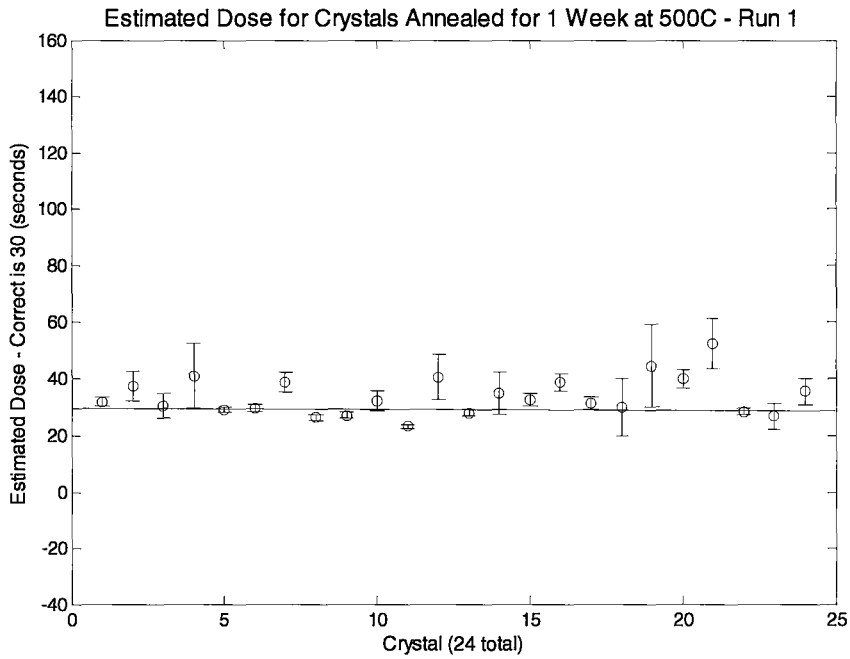

Figure 24: Estimated dose for crystals annealed for 1 week at 500°C – Run 2

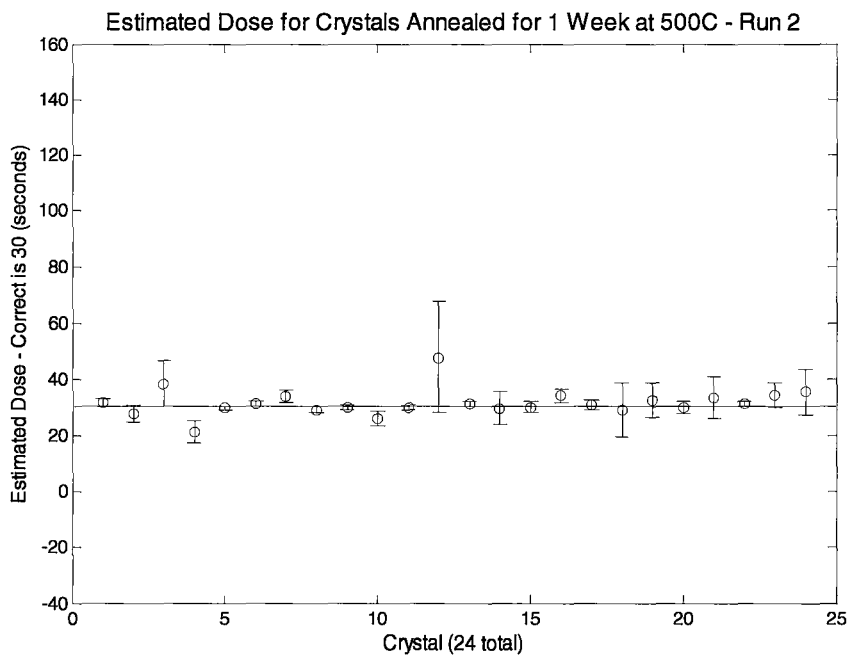

The number of crystals that recovered correct dose estimates within error is shown by treatment and OSL run in Figure 26. Except for the 300°C anneal treatment the crystals performed better in the second OSL run than in the first. The improvement was greatest for the 400°C and 500°C anneal treatments. This improvement was so great largely because of the very poor dose estimates from the first run, while the 200°C and 300°C treatments did not see such drastic improvements in results. Though the second run for the 200°C, 400°C, and 500°C all gave near the same proportion of correct dose estimates, examination of Figure 18, Figure 22, and Figure 24 reveal that the uncertainty of the dose estimates are far less for the 500°C run than in the other two treatments. The signal mean and two standard deviations of the treatment groups are shown in Figure 25. The mean signal for the 500°C treatment group is over twice that of any other anneal treatment, suggesting that a higher signal magnitude results in a lower estimated dose error. The two standard deviation error bars also increase in magnitude as the treatment temperature increases from 200°C to 500°C. This reflects the fact that some crystals are more readily sensitized at increased temperature than other crystals. This results in a greater range of signal magnitudes, though all crystals had an increase in peak signal after 500°C annealing. The standard deviation of signal magnitudes shown in Figure 25 also reveals that for some crystals the dose signal magnitude is below zero. This is due to subtraction of signal minus background, which for very low crystal signals, may produce a negative value.

Figure 25: Signal magnitudes for 1 week annealing treatments

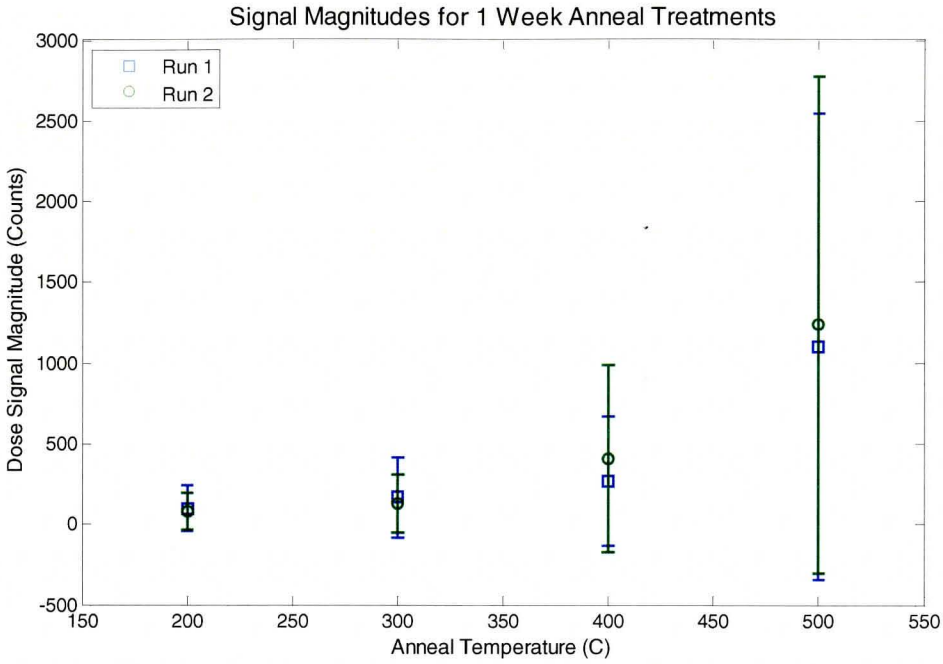

Figure 26: Dose estimate results after 1 week anneal treatments

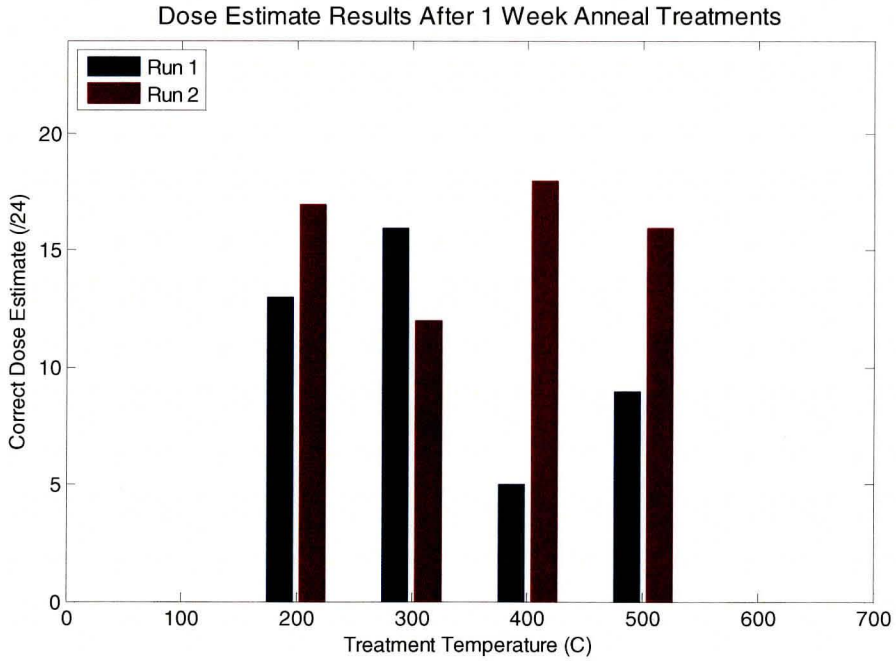

4.6 One week anneal at 500°C and 32 one hour heat treatment cycling

The previous anneal experiment revealed that the 500°C treatment created the highest sensitization, as observed from treatment temperatures ranging from 200°C to 500°C. Since the 500°C crystals also showed improvement in sensitivity and estimated dose results after one SAR protocol, it is clear that the SAR measurement process was continuing to improve the results. However, the SAR protocol involves heating the crystals to relatively low temperatures of 160°C for the pre-heat and 125°C during OSL measurement. Since the 500°C week long anneal resulted in the greatest sensitization it was possible that higher temperature cycling may induce greater sensitization than that created by the SAR protocol. To test this hypothesis, groups of 24 crystals first annealed to 500°C for 1 week, mimicking the anneal treatment of the previous experiment. The crystals were then separated into groups of 24 crystals and annealed 32 times for one hour at the temperatures 200°C, 300°C, 400°C, or 500°C. A total of 32 anneal cycles was chosen because it is the same number of heating cycles used in the SAR protocol for a single run. Once the thermal treatments were completed the crystals were subjected to two SAR runs. For the one week anneal and cycling experiment, groups of 24 crystals were used in each treatment. The x-axis of the ED plots shows the number of crystals providing dose estimates out of the 24 treated. ED results for all runs and treatment groups are shown in Figure 27 to Figure 34. The most striking difference between the cycled crystals and the previous experiments is the relatively small error associated with most estimated doses. It is also obvious that most ED are in the range of 25-35 seconds for all treatment groups on both runs, with only a few crystals in each treatment falling

outside of this range. The best results are for the 200°C and 300°C second runs which not only had a good number of correct ED within uncertainty, but for the incorrect ED the results were often near 30 with a small error. For all annealed and heat cycled crystals the 30 second irradiation equals a dose of 2.51 Gy.

Figure 27: Treated for 1 week at 500°C and 32 one hour anneals at 200°C - Run 1

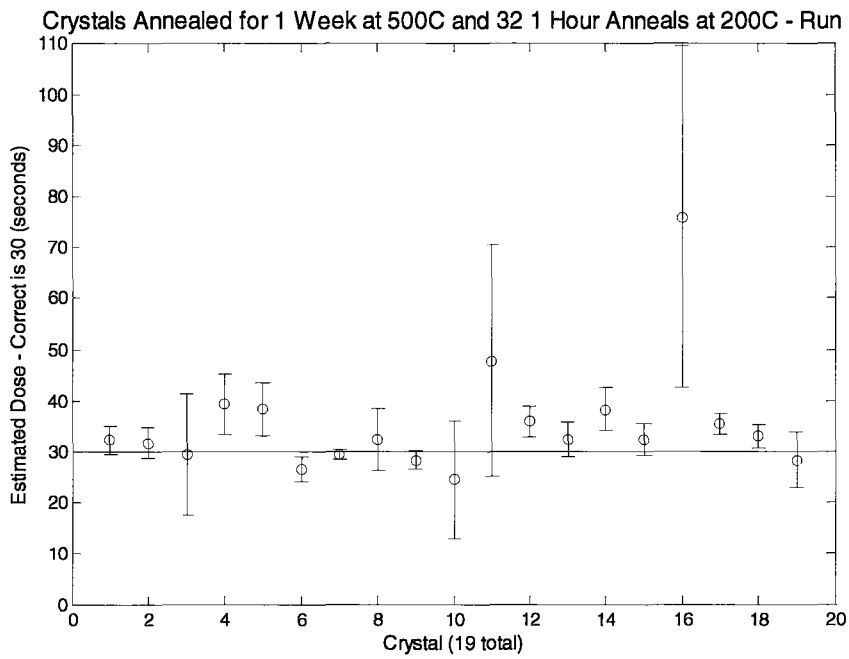

Figure 28: Treated for 1 week at 500°C and 32 one hour anneals at 200°C - Run 2

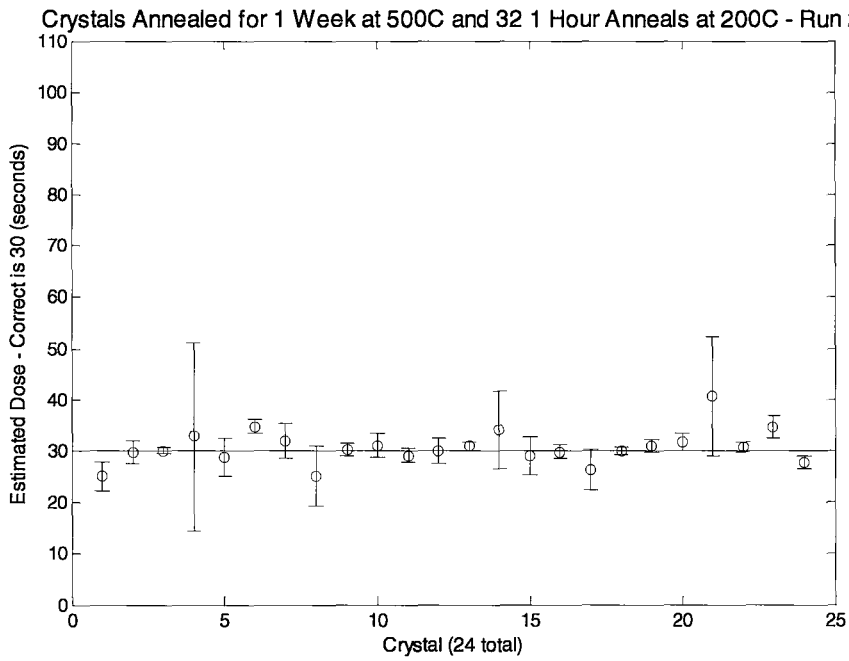

Figure 29: Treated for 1 week at 500°C and 32 one hour anneals at 300°C - Run 1

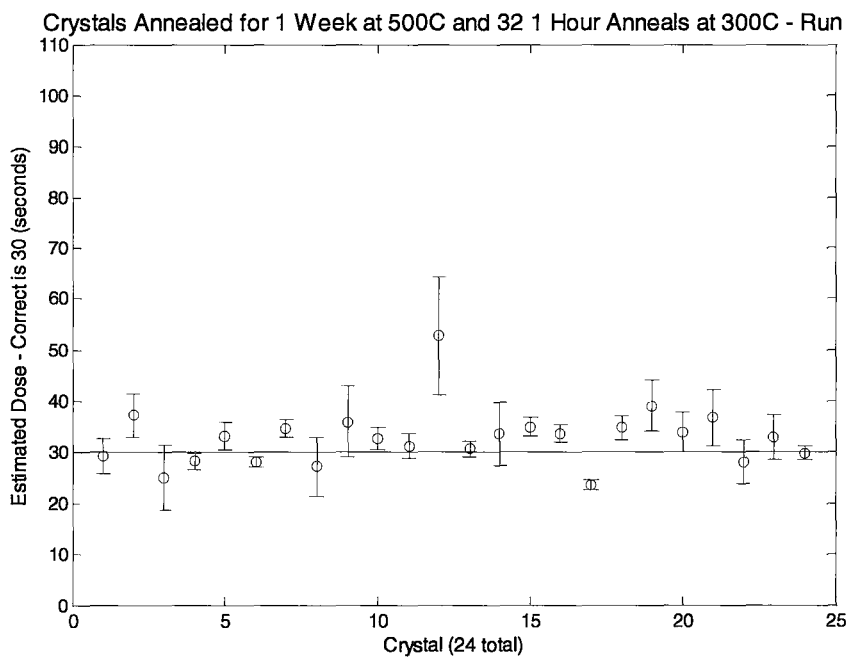

Figure 30: Treated for 1 week at 500°C and 32 one hour anneals at 300°C - Run 2

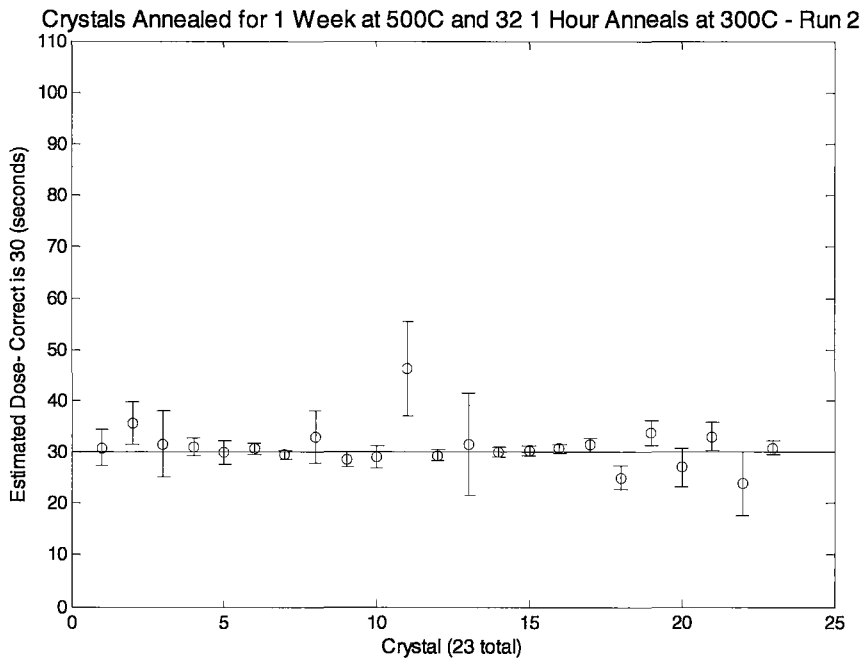

Figure 31: Treated for 1 week at 500°C and 32 one hour anneals at 400°C - Run 1

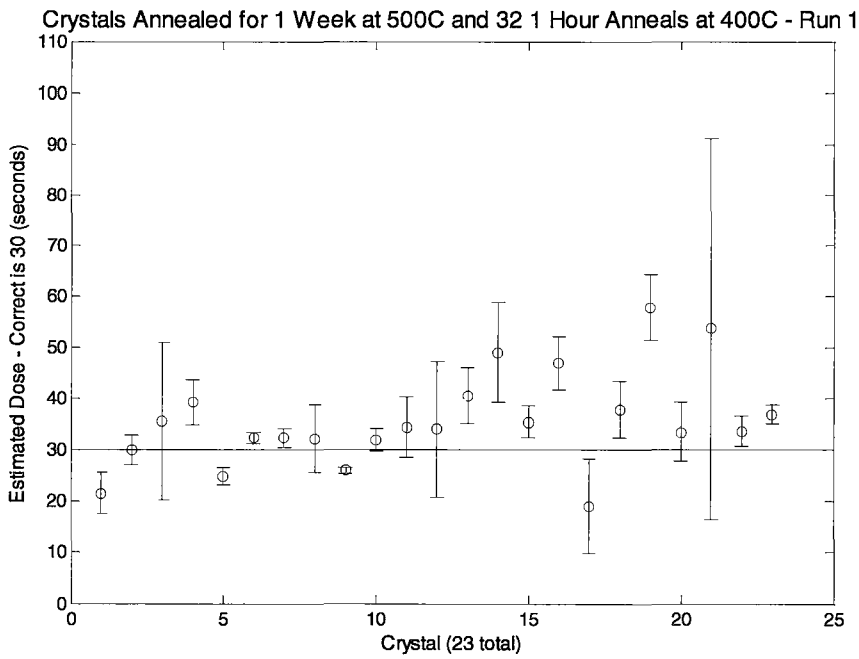

Figure 32: Treated for 1 week at 500°C and 32 one hour anneals at 400°C - Run 2

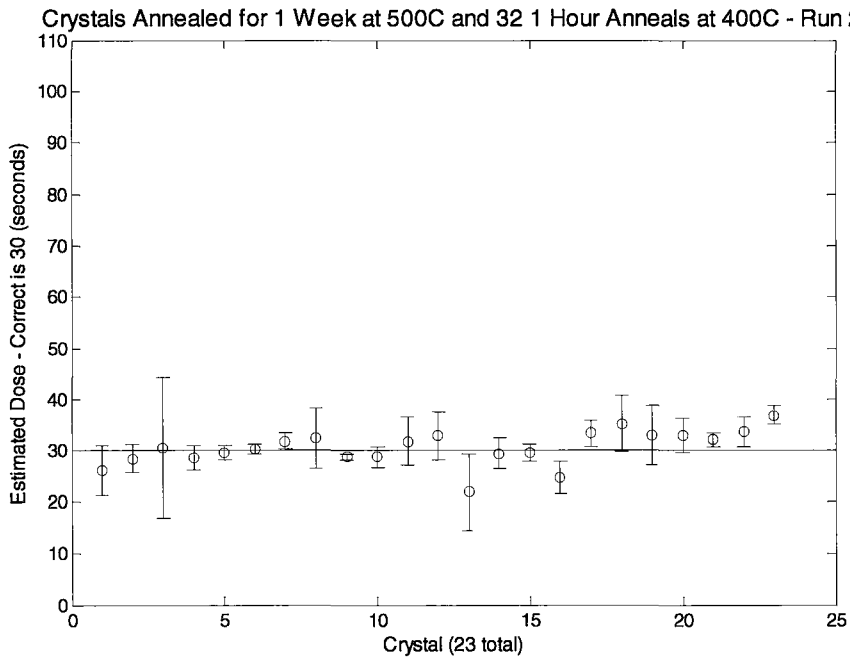

Figure 33: Treated for 1 week at 500°C and 32 one hour anneals at 500°C - Run 1

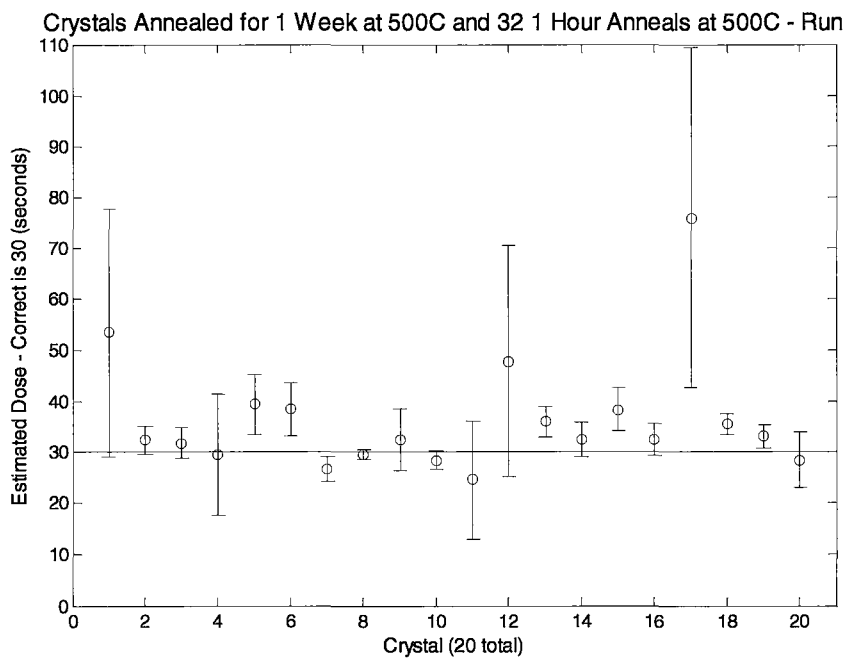

Figure 34: Treated for 1 week at 500°C and 32 one hour anneals at 500°C - Run 2

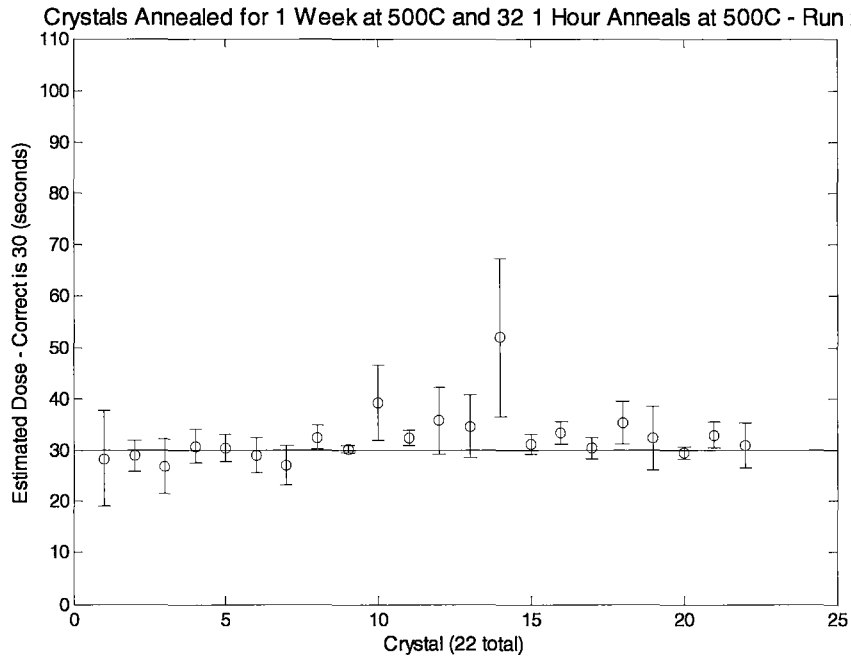

Sensitization enhancement due to anneal cycling was not observed with increasing temperature; which was expected from the results of the one week anneals presented in section 4.3. In fact, as shown in Figure 35 and Figure 36, the best results and the highest signal magnitudes were for the 200°C cycled crystals with the results becoming worse as the cycle temperature was increased (although the variation in signal magnitudes was lowest for the 500°C cycled crystals). This result was unexpected but does not contradict the observation that lower temperature cycling during the SAR protocol sensitizes the crystals and improves their dose recovery characteristics. In fact the temperatures used for the SAR protocol in this work were 125°C during OSL measurement and 160°C during the pre-heat. Both of these temperatures were closer to the 200°C treatment group that was the most successful in this experiment. The reason

that lower temperature cycling causes greater sensitization than higher temperature cycling after a 500°C anneal is unclear, particularly since over one week time periods higher temperature anneals were shown to induce greater sensitization than lower temperature anneals. Speculatively, there may be different processes occurring at lower and higher temperatures which affect the luminescence process. In the high temperature case these processes may have a relatively long lifetime which was not strongly affected by the repeated short term anneals performed here. The process underlying low temperature sensitization may act rapidly, as observed during the SAR protocol when heating only takes place for 100 seconds. With this dynamic the repeated one hour heat cycles would have had a stronger influence on the low temperature sensitization than the high temperature sensitization.

Figure 35: Crystals annealed at 500°C for 1 week and cycled 32 times for 1 hour

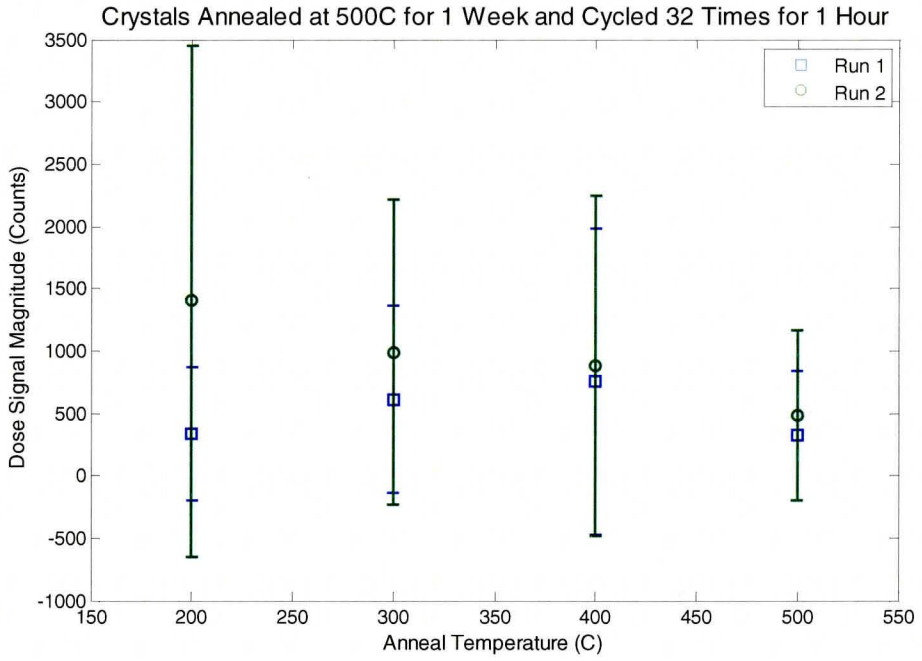

Figure 36: Dose estimate results after 500°C anneal for 1 week and 32 1 hour cycles

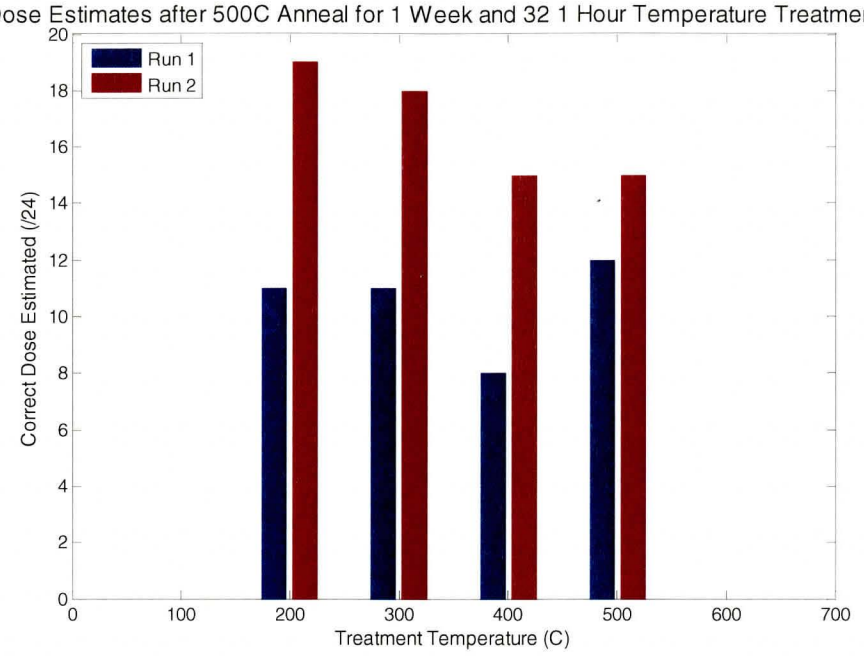

4.7 Thirty two one hour heat treatment cycles

The improvement in estimated dose and increase in sensitivity observed after the first SAR protocol suggests that heating, irradiation, and light stimulation sensitize the crystals and improve their dosimetric properties. To test the extent to which heat cycling (without preannealing) on its own can improve sensitization, a total of 24 crystals per temperature were subjected to 32 one hour heat cycles at 200°C, 300°C, 400°C, or 500°C. Two runs were performed per treatment group. The results are shown from Figure 37 to Figure 44. For the cycling experiment, groups of 24 crystals were used in each treatment. The x-axis shows the number of crystals providing dose estimates out of the 24 treated. For all runs the largest range in estimated dose errors were associated with the 200°C cycled crystals, which makes this treatment undesirable due to its very low precision. The highest precision was from the second run of the 400°C cycled crystals.

For this treatment group, shown in Figure 42, all estimated doses but two were in the range of 25-35 seconds, which is an excellent result with the ED quite close to the correct value of 30. This high precision is likely caused by the E' centre being filled with a free electron, thus preventing the oxygen vacancy from acting as a non-luminescent recombination centre. The cycled crystals still did not perform as well as the crystals that received a one week 500°C anneal and then the cycling treatment. A large number of crystals were outside of the 25-35 second ED range for all runs. The best results from this cycling experiment were for the 300°C and 400°C treatment groups, although the uncertainty in ED for most crystals here is greater than for the cycled crystals that also received a one week anneal. For all heat cycled crystals the 30 second irradiation equals a dose of 2.51 Gy.

Figure 37: Crystals treated with 32 1 hour anneals at 200°C – Run 1

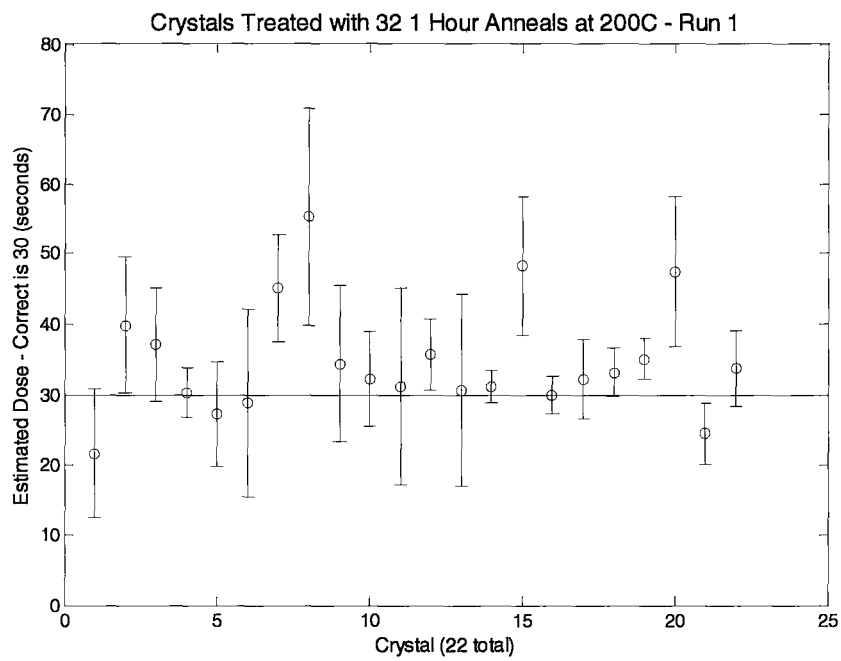

Figure 38: Crystals treated with 32 1 hour anneals at 200°C – Run 2

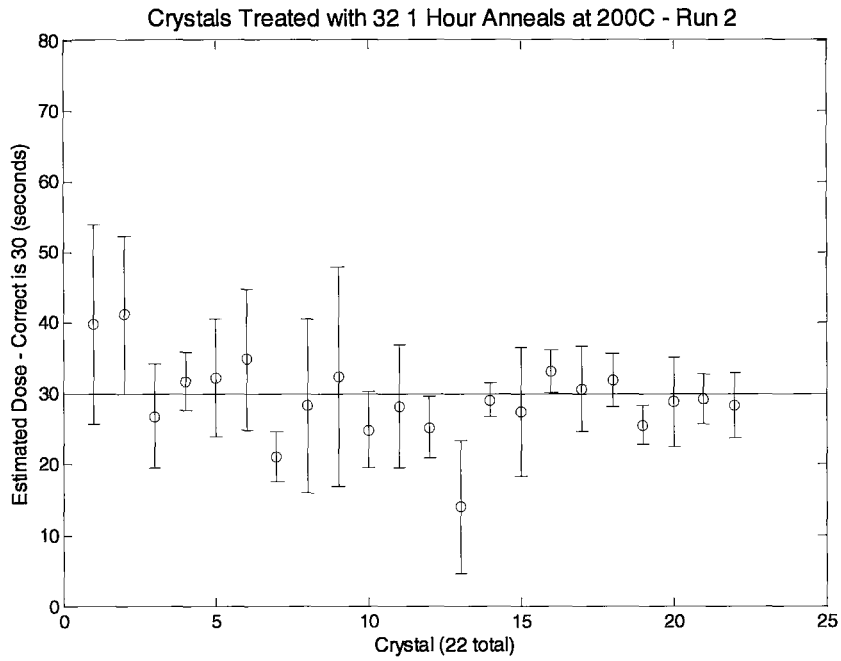

Figure 39: Crystals treated with 32 1 hour anneals at 300°C – Run 1

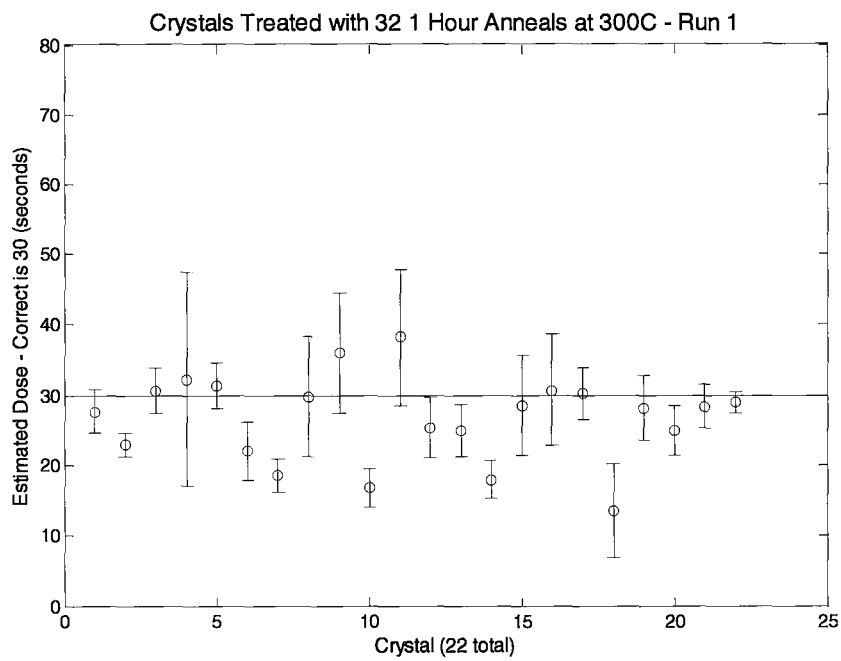

Figure 40: Crystals treated with 32 1 hour anneals at 300°C – Run 2

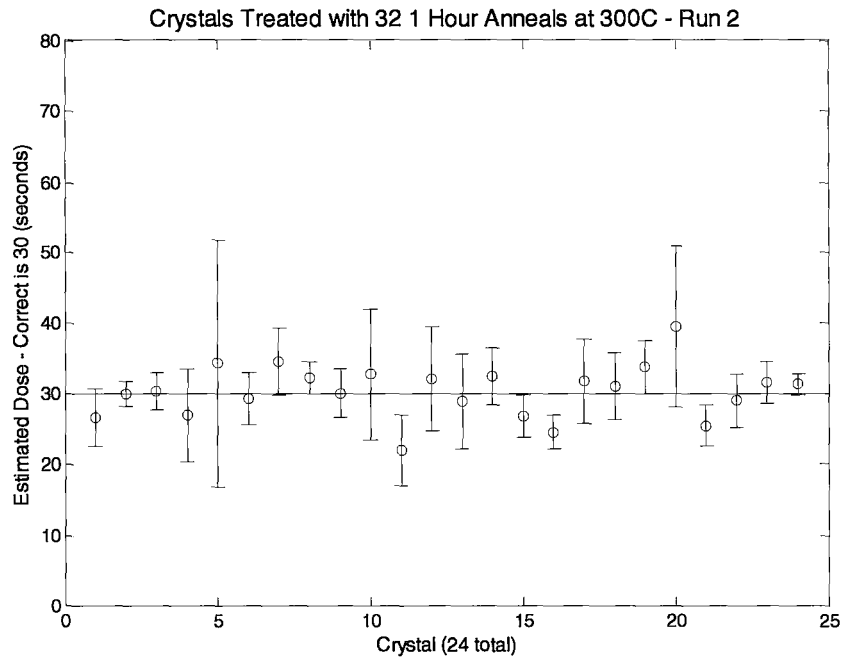

Figure 41: Crystals treated with 32 1 hour anneals at 400°C – Run 1

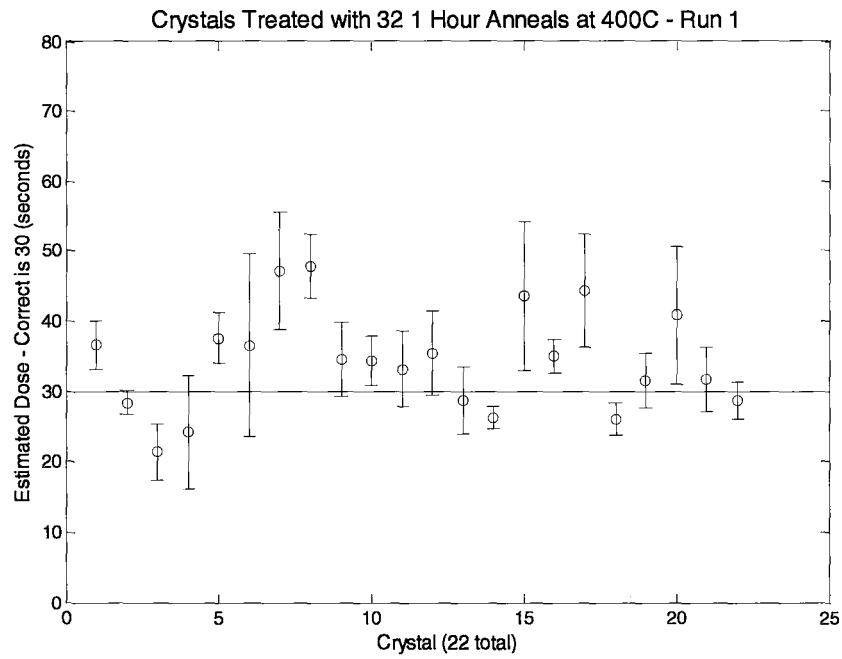

Figure 42: Crystals treated with 32 1 hour anneals at 400°C – Run 2

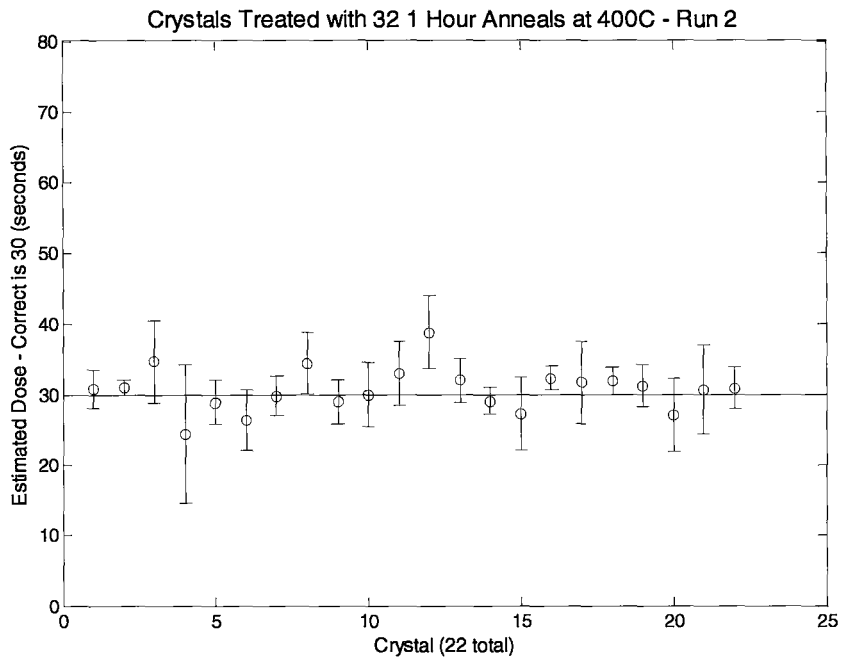

Figure 43: Crystals treated with 32 1 hour anneals at 500°C – Run 1

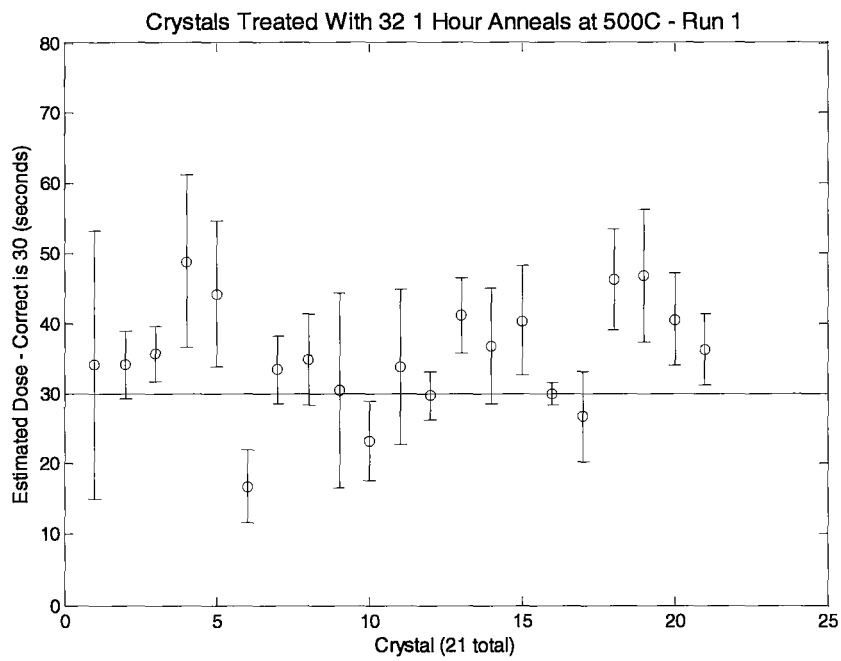

Figure 44: Crystals treated with 32 1 hour anneals at 500°C – Run 2

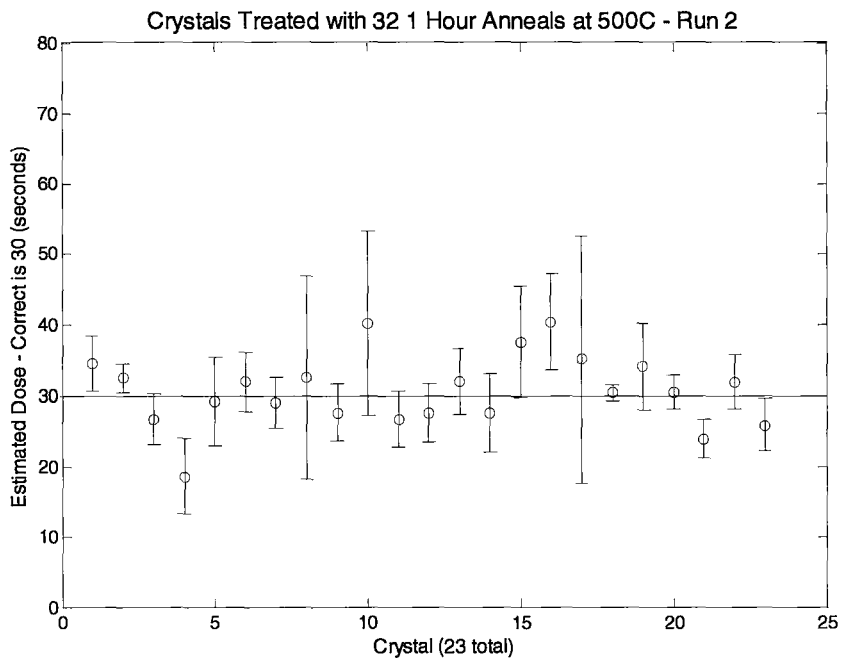

The effects of heat cycling at 200°C, 300°C, 400°C, and 500°C show less of a dependence upon temperature than when the crystals are cycled after a one week 500°C anneal. Figure 45 presents the average signal magnitude and two standard deviations for the cycled crystals. In this case the highest average signal magnitudes are for the 300°C and 400°C treatments as opposed to the highest or lowest temperatures tested in the experiment. The number of crystals with a correct ED, shown in Figure 46, also reflects this trend where the 300°C and 400°C treatments are the most successful in the second OSL run. The signal magnitude for all cycled crystals is relatively small compared to the signal magnitudes obtained by long duration high temperature anneals. Comparison of Figure 35 and Figure 45 reveals the importance of a high temperature anneal before

thermal cycling for the 200°C treatment group. After the 500°C one week anneal followed by 32 thermal cycles at 200°C this group had the highest signal magnitudes of all treatment groups examined (about 1500 counts for run 2). When these crystals were only subjected to the 200°C thermal cycling the signal magnitude was very low, being on average approximately 300 counts for run 2. Examination of the 200°C treatment in Figure 46 also reveals that the ED estimates did not improve as much as the other temperature groups from run 1 to run 2.

Figure 45: Signal magnitude for crystals cycled 32 times for 1 hour

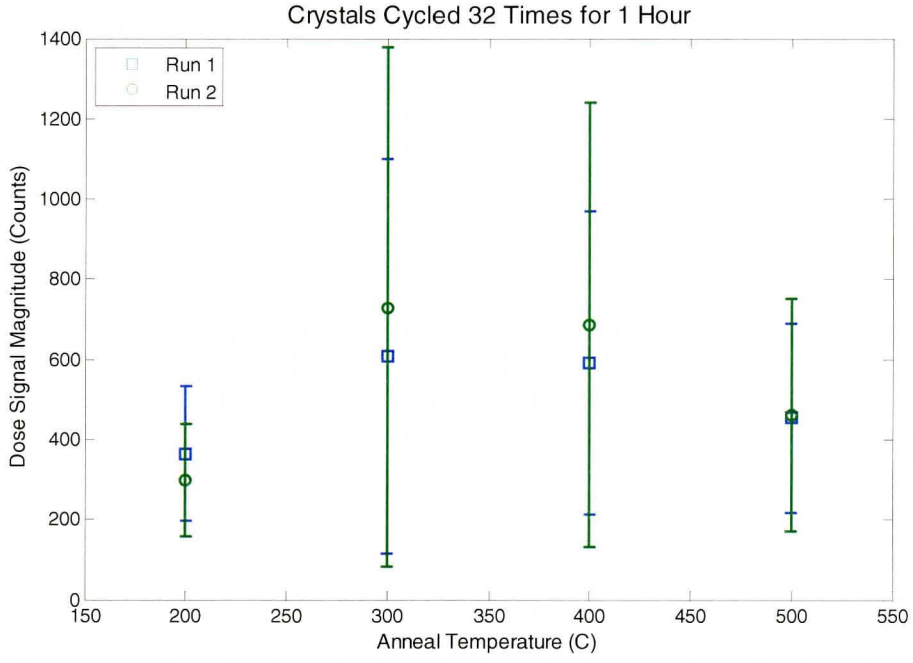

Figure 46: Dose estimate results for crystals annealed for 1 hour 32 times

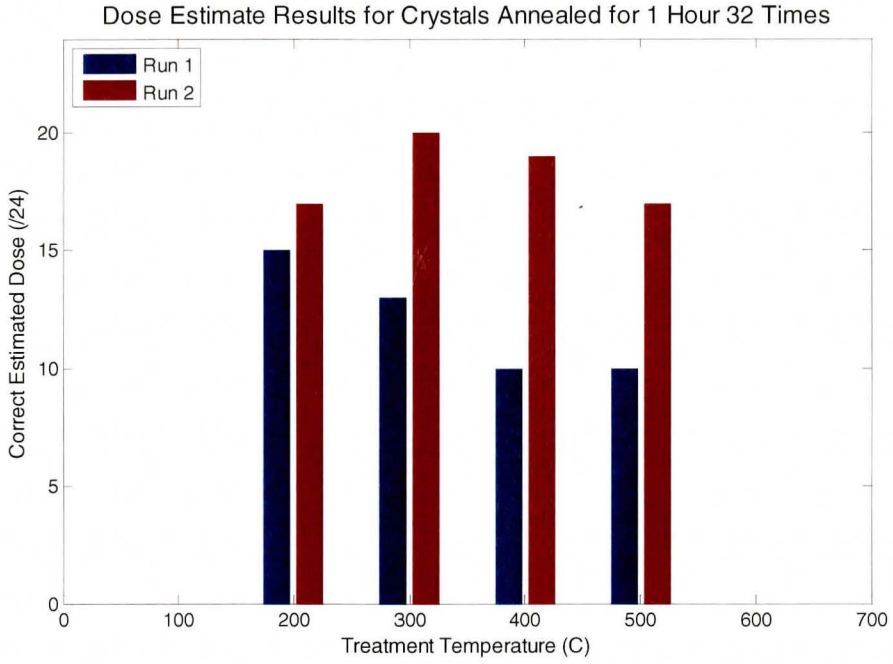

4.8 800°C one week heat treatment – 2.5 Gy regeneration dose

All annealing treatments previously considered were up to a maximum of 500°C. This was because of a concern that anneals above this temperature may affect the oscillatory properties of the quartz crystal, thus rendering them useless as timekeepers (King and Fraser, 1961). The study by King and Fraser (1961) involved measuring the performance of the quartz resonator while held at elevated temperatures, no studies were found that examined the performance of quartz oscillators after such annealing and cooling. Therefore, while poor performance is a problem for quartz oscillators held at temperatures beyond 500°C they will likely function well once cooled back to room temperature (Schwarcz and Rink, Personal Communication). In an effort to increase the sensitivity of the quartz as much as possible while in the range of 20°C to 1200°C, anneals were carried out at 800°C, the temperature known to induce greatest sensitization

(Bøtter-Jensen, Larsen et al., 1995). Estimated dose results for three OSL runs completed on the same aliquots are shown in Figure 47, Figure 48, and Figure 49. For the 800°C annealing experiment, groups of 24 crystals were used in each treatment. The x-axis shows the number of crystals providing dose estimates out of the 24 treated. There is a vast underestimation of dose in nearly all crystals for the first OSL run, shown in Figure 47. This underestimation is still seen in the second OSL run and to a lesser extent in the third OSL run. The uncertainty in ED is greatly reduced for all crystals on all runs and is often only a fraction of a second, far lower than any other treatment tested so far. For the 800°C annealed crystals the 30 second irradiation equals a dose of 2.50 Gy.

Figure 47: Estimated Dose for Crystals Annealed for 1 Week at 800C – Run 1

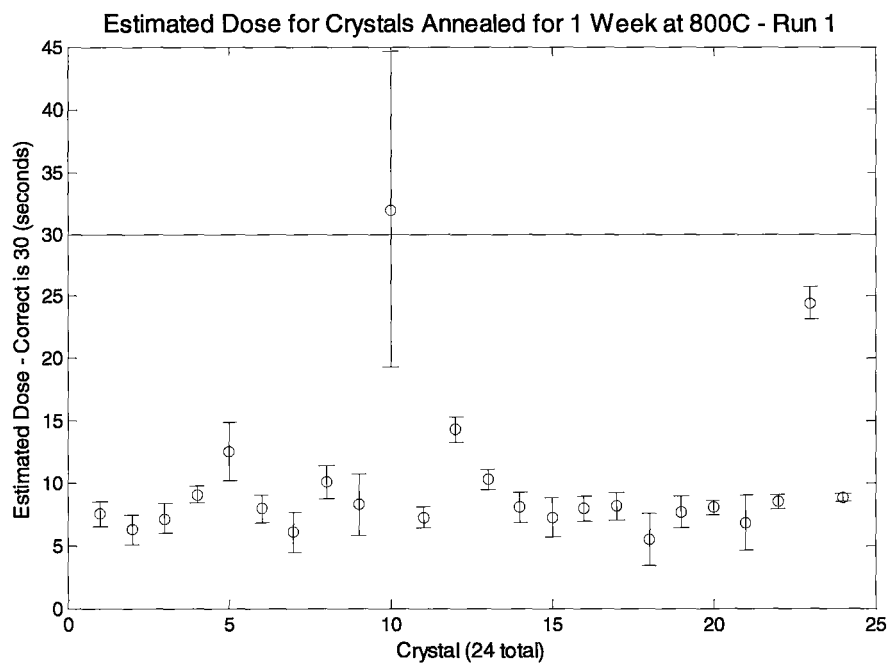

Figure 48: Estimated Dose for Crystals Annealed for 1 Week at 800C – Run 2

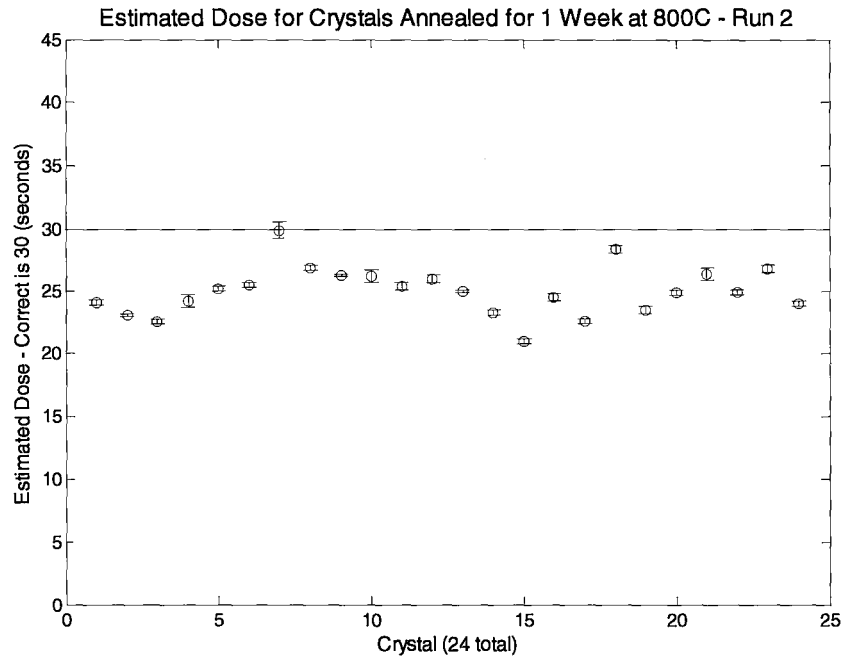

Figure 49: Estimated Dose for Crystals Annealed for 1 Week at 800°C – Run 3

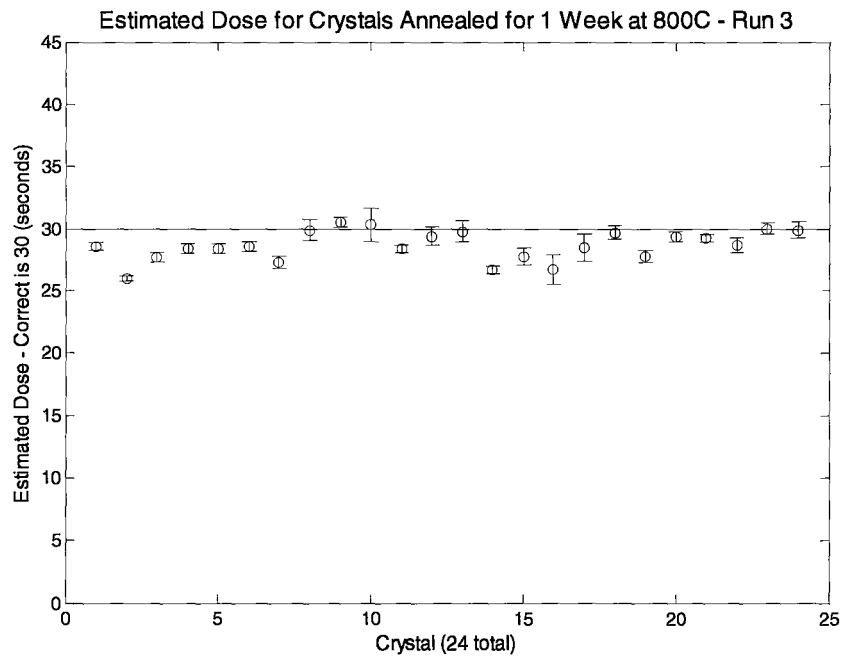

While the ED shows significant improvement over other treatments performed on the quartz, the improvement in signal magnitude is even more pronounced. Examination of Figure 51, Figure 52, and Figure 53 shows an increase in signal magnitude of approximately three orders of magnitude for nearly all aliquots from the first to the second run; and the signal continued to increase on the third OSL run. Figure 54 shows the average signal magnitude with two standard deviations for all crystals for the three runs. This figure also makes it clear that there is a large increase in crystals sensitivity after each run. Though the goal of this research is to increase the sensitivity of the crystals, this large increase in sensitivity over the three runs can be problematic for dose estimation calculations. The SAR protocol seeks to compensate for sensitivity change through the use of a test dose, this also rests on the assumption that little to no sensitivity change is occurring from the regeneration dose to the subsequent test dose, or that the sensitivity change is linear for all signal and test doses throughout the entire SAR protocol. The large sensitivity increase observed between Run 1 and Run 2 when compared to the sensitivity change from Run 2 to Run 3 does not support this assumption. There is a far greater increase in sensitivity from Run 1 to Run 2 than from Run 2 to Run 3. This suggests that throughout the three runs the sensitivity change is non-linear and therefore within each run the sensitivity change may not be fully corrected by the use of a test dose in the SAR protocol. This would result in underestimation of the estimated dose since the ratio of regeneration signal to tests dose would be smaller at the beginning of the SAR protocol than at the end. Table 3, Table 4, and Table 5 presents data from aliquot 24 in runs 1, 2 and 3. This aliquot is representative of others in the

treatment group which significantly underestimated the ED in run 1 and improved its results in the later two runs. It is apparent that the initial dose to be recovered for run 1 only provided a total of 4352 counts above background as compared to the test signal of 34,293. This relatively low initial sensitivity for the 30 second irradiation resulted in a low ratio of regeneration/test dose signal which was strongly influenced by background counts. The increase in test dose was also non-linear. In run 1 some test doses nearly tripled in subsequent measurements while others increased by a half or less. The large variation in sensitivity change occurring over the course of the SAR protocol resulted in poor dose estimations for the first run when crystal sensitivity was most volatile. For run 3, whose count data is shown in Table 5, the test dose counts were not nearly as volatile. Increases in the order of a few thousand counts, out of the test dose total of over a million, is relatively stable compared to the tripling of test dose counts observed in run 1. This led to the marked improvement in dose estimate accuracy seen for run 3. Figure 50 presents the recycling ratios of all crystals subjected to 800°C for one week for runs 1, 2, and 3. There is a vast improvement as the runs progress, showing that for the third run most recycling ratios are in the ideal range of 0.9 to 1.1. This indicates that the sensitivity change of the crystals is becoming more stable with subsequent runs.

Table 3: Signal magnitudes for aliquot 24 treated to 800°C for 1 week – Run 1

Irradiation Time (seconds)	Regeneration Signal Magnitude (Counts)	Test Dose Signal Magnitude (Counts)	Regeneration/Test Dose
30	4,352	34,293	0.126
15	19,956	97,872	0.203
25	62,645	194,495	0.321
35	141,579	305,607	0.462
45	259,972	449,709	0.577
55	401,687	600,339	0.669
0	4,912	672,131	0.007
25	389,067	774,657	0.501

Table 4: Signal magnitudes for aliquot 24 treated to 800°C for 1 week – Run 2

Irradiation Time (seconds)	Regeneration Signal Magnitude (Counts)	Test Dose Signal Magnitude (Counts)	Regeneration/Test Dose
30	495,436	870,383	0.569
15	363,274	950,531	0.382
25	534,261	887,880	0.601
35	698,497	959,198	0.728
45	840,105	997,741	0.842
55	982,392	1,055,287	0.931
0	11,793	1,077,786	0.011
25	717,952	1,173,559	0.611

Table 5: Signal magnitudes for aliquot 24 treated to 800°C for 1 week – Run 3

Irradiation Time (seconds)	Regeneration Signal Magnitude (Counts)	Test Dose Signal Magnitude (Counts)	Regeneration/Test Dose
30	839,234	1,133,883	0.740
15	544,905	1,143,592	0.476
25	798,038	1,194,856	0.667
35	1,059,697	1,382,350	0.766
45	1,247,884	1,316,115	0.948
55	1,361,044	1,336,109	1.019
0	19,627	1,384,025	0.014
25	1,003,309	1,430,876	0.701

Figure 50: Recycling ratios for each crystal by run

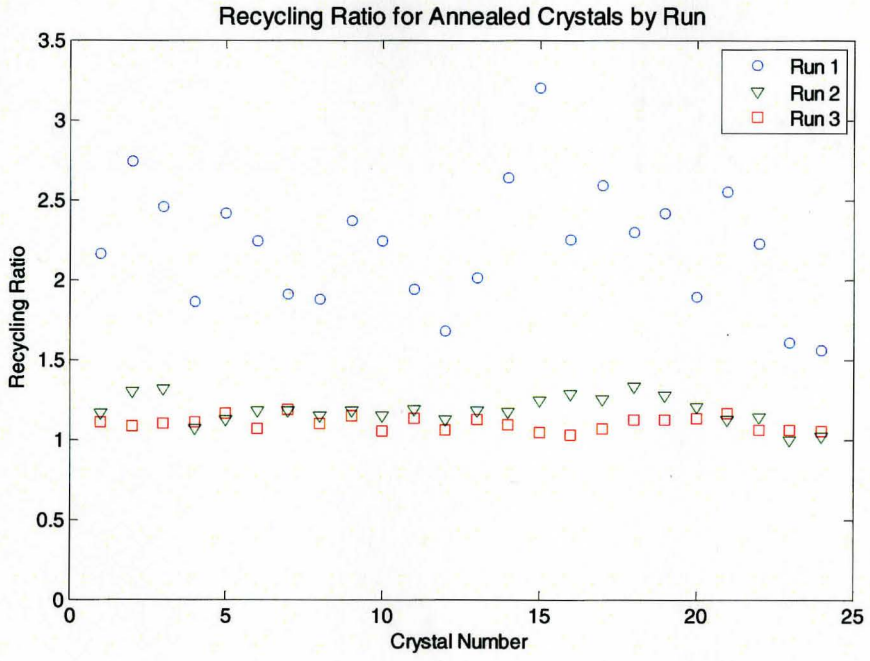

Figure 51: Signal magnitude for 1 week at 800°C annealed crystals – Run 1

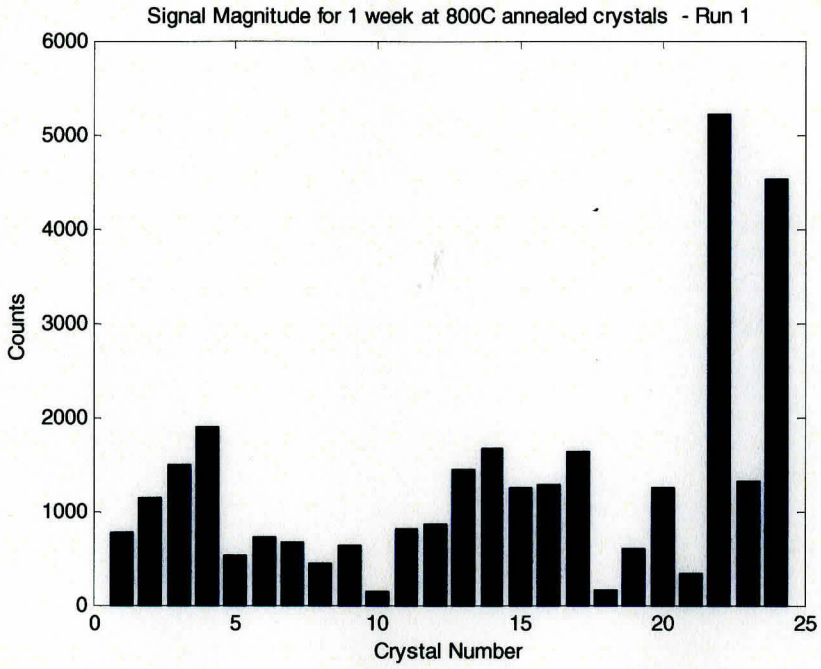

Figure 52: Signal magnitude for 1 week at 800°C annealed crystals – Run 2

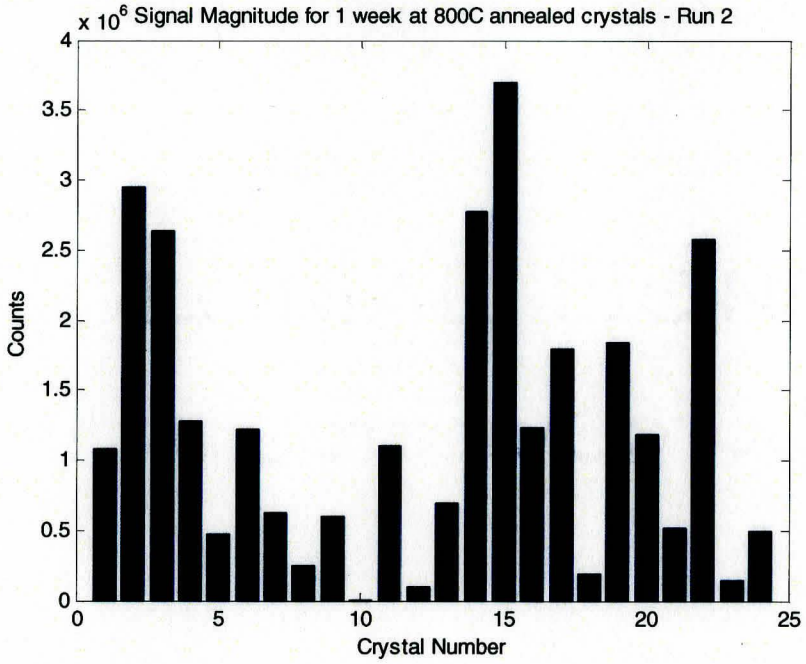

Figure 53: Signal magnitude for 1 week at 800°C annealed crystals – Run 3

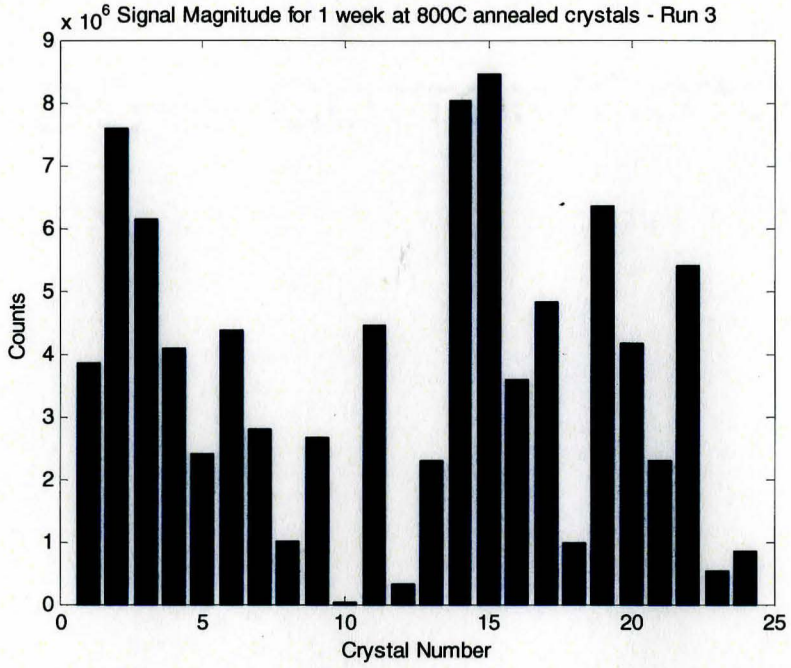

Figure 54: Average counts by run for 800°C annealed crystals. 2.5 Gy regeneration

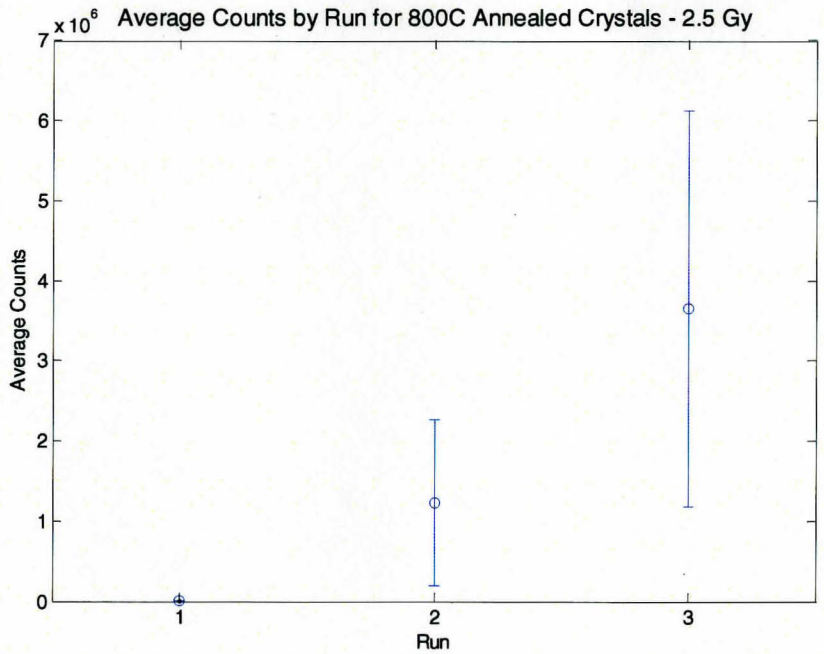

4.9 800°C one week heat treatment – 0.5 Gy regeneration dose

The previous 30 second irradiation corresponds to a dose of approximately 2.50 Gray, this is a relatively large dose for an individual to receive; though it should be noted that the biological effects would still be dependent on the radiation quality factor. In order to increase the usefulness of OSL in synthetic quartz, this method should be able to assess doses in the range of less than one Gray. 0.5 Gy was chosen as the dose to be investigated since it required irradiations of 6 seconds. The regeneration doses required to bracket this was at its shortest a 4 second irradiation, which is near the threshold of reliable dose delivery for the Risø system used. Only crystals annealed to 800°C were used to assess the 0.5 Gy dose because of their high sensitivity. Estimated dose results are shown in Figure 55, Figure 56, and Figure 57 for crystals subjected to three OSL runs. For the 800°C anneal experiment, groups of 24 crystals were used in each treatment. The x-axis shows the number of crystals providing dose estimates out of the 24 treated.

Comparison of the first OSL run from the 6 second and 30 second regeneration doses, shown in Figure 47 and Figure 55, reveals that the underestimation in the aliquots at the 30 second dose is not as pronounced in the 6 second regeneration dose. Also, despite being a much smaller dose, the 6 second regeneration does not have large associated uncertainties. This is due to the strong OSL signal measured, which indicates that the crystals are very sensitive and would be able to resolve much lower doses if they could be accurately delivered using a lower dose rate Risø system. Runs 2 and 3 shown in Figure 56 and Figure 57 also show that these crystals act as excellent dosimeters. Both runs show improvement over run 1 and show a decrease in uncertainty of the estimated

dose. For the third run 18/24 crystals had their estimated dose within the true value by half a second of irradiation. This half-second error represents a dose of 0.04 Gy off the true value of 0.5 Gy, which is approximately 8.4% of the given dose. All other estimated doses were off by a maximum of one second. Figure 58 presents the average signal magnitude and two standard deviations for all crystals in run one, two and three. Even at a relatively low dose of 0.5 Gy average counts for run three are quite high, far above background, thereby reducing the dose estimation error.

Figure 55: Estimated Dose for Crystals Annealed for 1 Week at 800°C – Run 1

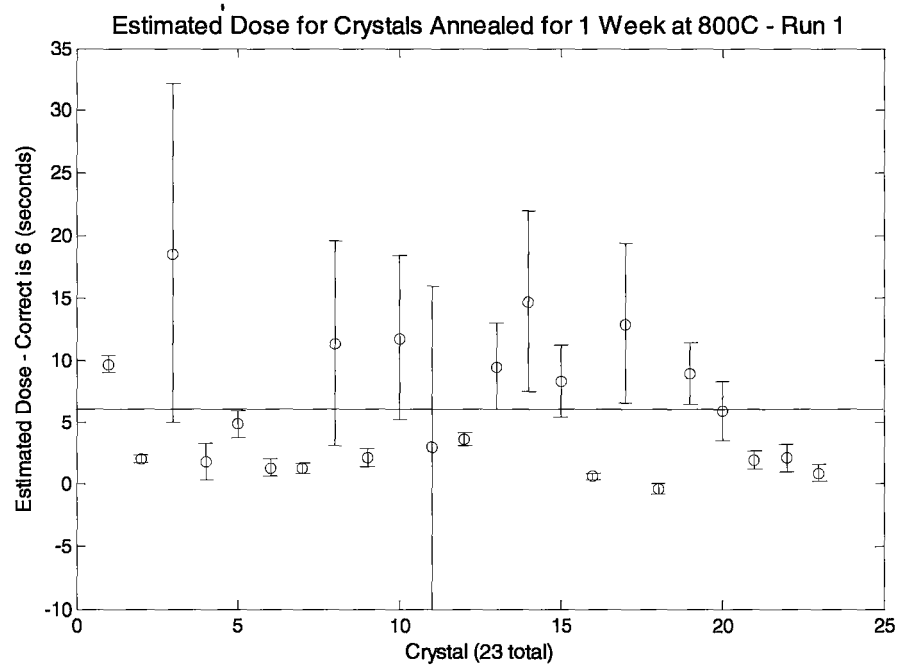

Figure 56: Estimated dose for crystals annealed for 1 week at 800°C – Run 2

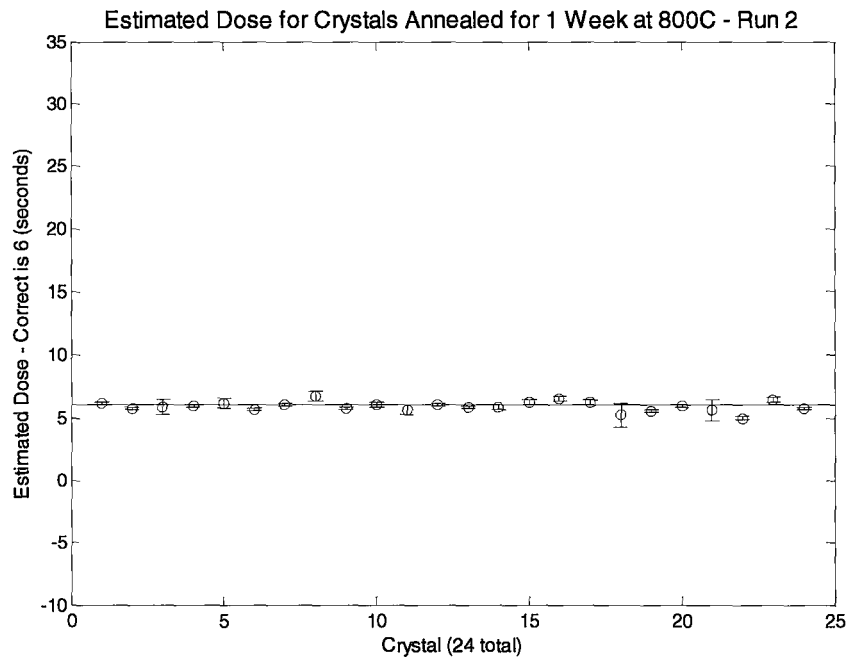

Figure 57: Estimated dose for crystals annealed for 1 week at 800°C – Run 3

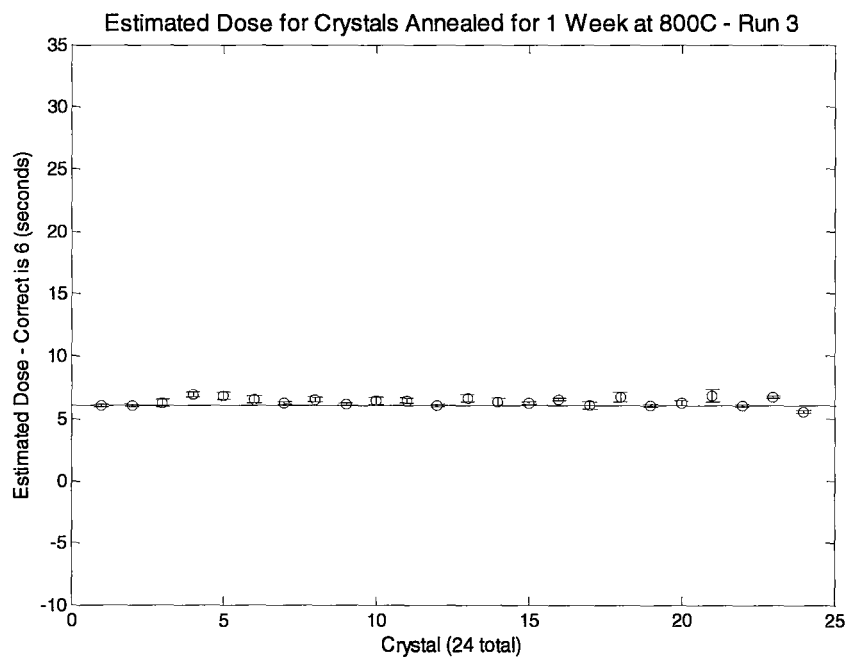

Figure 58: Average counts by run for 800°C annealed crystals - 0.5 Gy

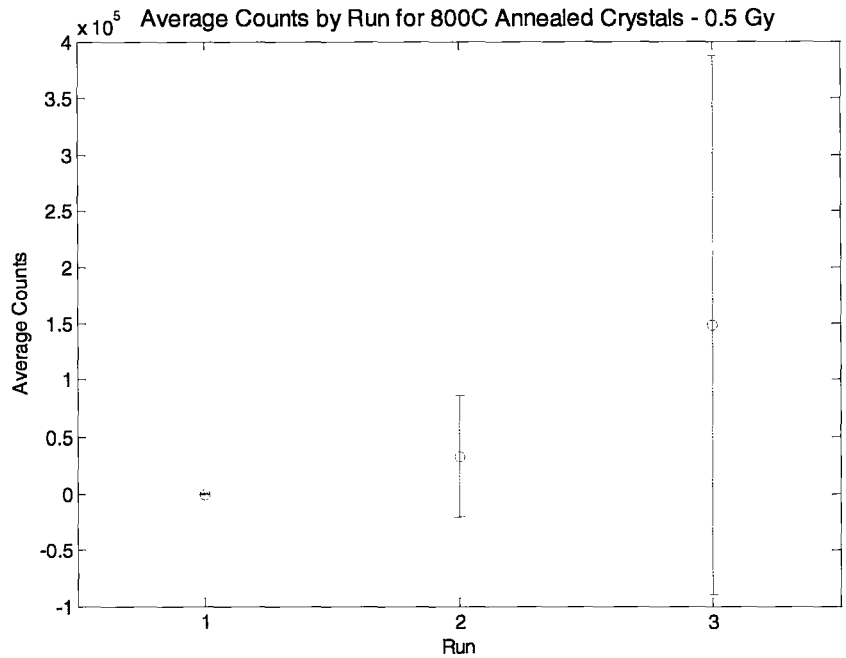

4.10 800°C one week heat treatment – larger sample reproduction of results

A second set of crystals was used to validate and reproduce the OSL sensitization observed at the 0.5 Gy dose by the 800°C anneal treatment. The number of crystals treated was doubled to 48; all other aspects of the protocol remained the same. The x-axis shows the number of crystals providing dose estimates out of the 48 treated. The results of the three runs are presented in Figure 59, Figure 60 , and Figure 61. As previously observed with the 24 crystal group, the ED and associated error improves dramatically from the first to the second run with further improvement on the third OSL run. By the third OSL run 43 out of the 48 crystals gave ED estimates in the range of 5.8 to 6.2 seconds within uncertainty, which represents an error of 3% from the correct dose estimate. The other 5 crystals not in this error range were at the most 0.6 seconds from the correct ED of 6 seconds, representing a maximum error of 10% for all crystals.

Figure 59: Estimated dose for crystals annealed for 1 week at 800°C – Run 1

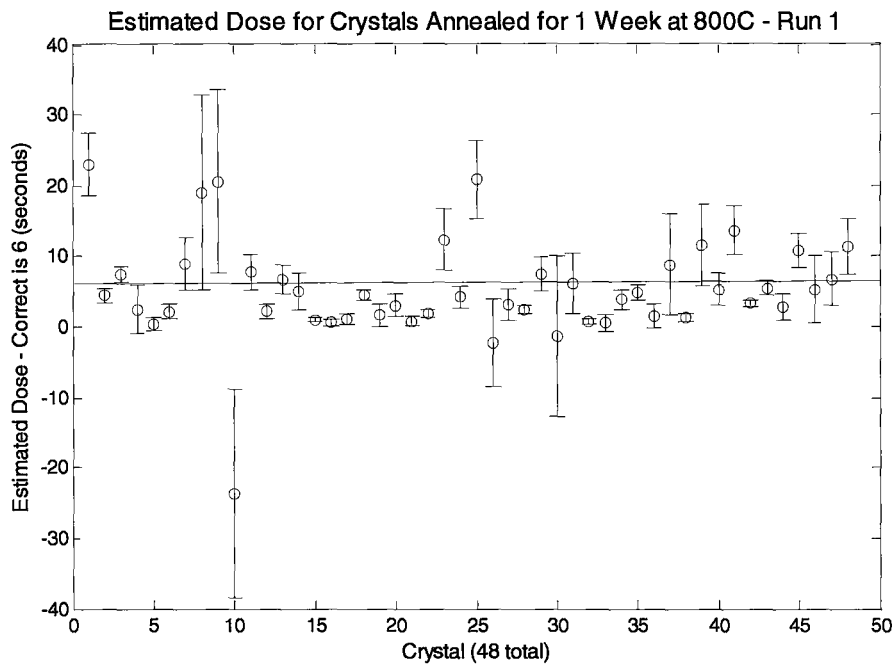

Figure 60: Estimated dose for crystals annealed for 1 week at 800°C – Run 2

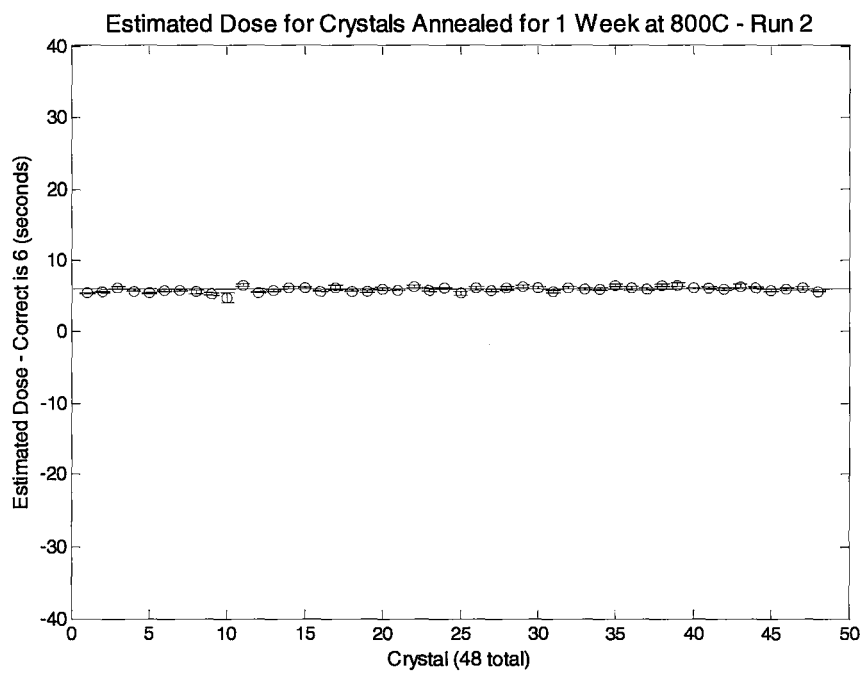

Figure 61: Estimated dose for crystals annealed for 1 week at 800°C – Run 3

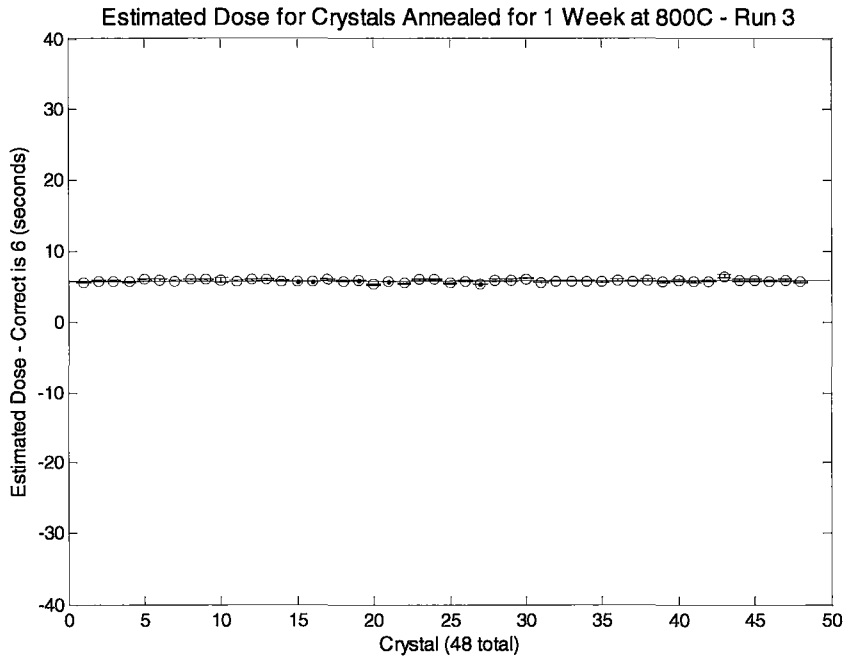

The improvement in ED was expected from the observed increase in signal magnitude from the first to the third OSL run. The signal magnitudes for all crystals for run 1, run 2, and run 3 are shown in Figure 62, Figure 63, and Figure 64 respectively. The average signal magnitude and two standard deviations for all crystals in runs 1, 2 and 3 are shown in Figure 65. The largest increase is from the first run to the second run, where the signal magnitudes increase from a maximum of near 500 counts to a maximum of approximately 110,000 counts. Even with the large increase in signal magnitude exhibited by some crystals, others do not respond with such a dramatic increase in sensitivity. Crystal 10 for all three runs had both the lowest counts and the largest error in ED. Despite this, for crystal 10 there was still a marked improvement in the dose estimate from the first to the third OSL run. This suggests all crystals can become well behaved dosimeters after an 800°C anneal and three SAR protocol runs.

Figure 62: Signal magnitudes for 1 week anneals at 800°C – Run 1

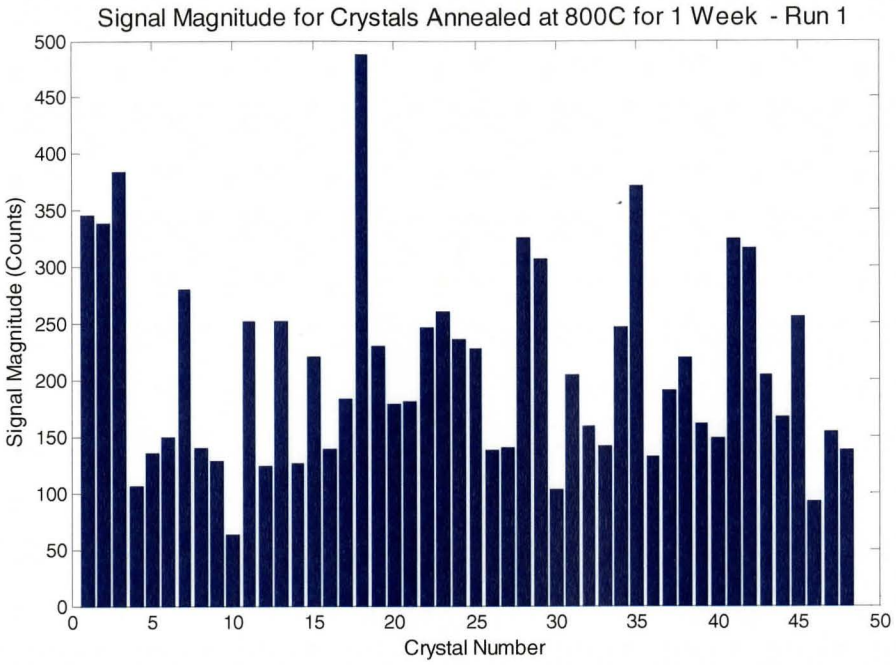

Figure 63: Signal magnitudes for 1 week anneals at 800°C – Run 2

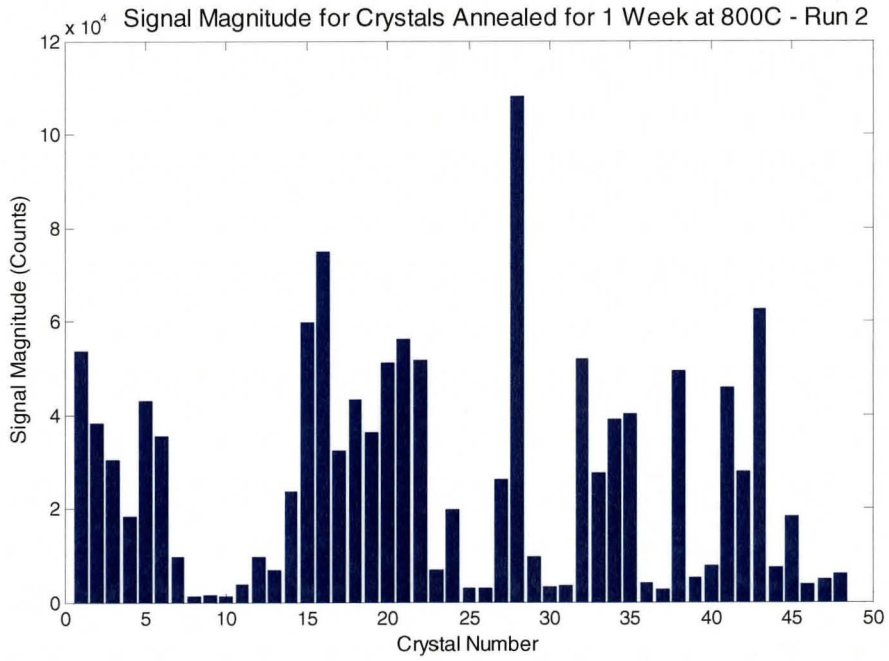

Figure 64: Signal magnitudes for 1 week anneals at 800°C – Run 3

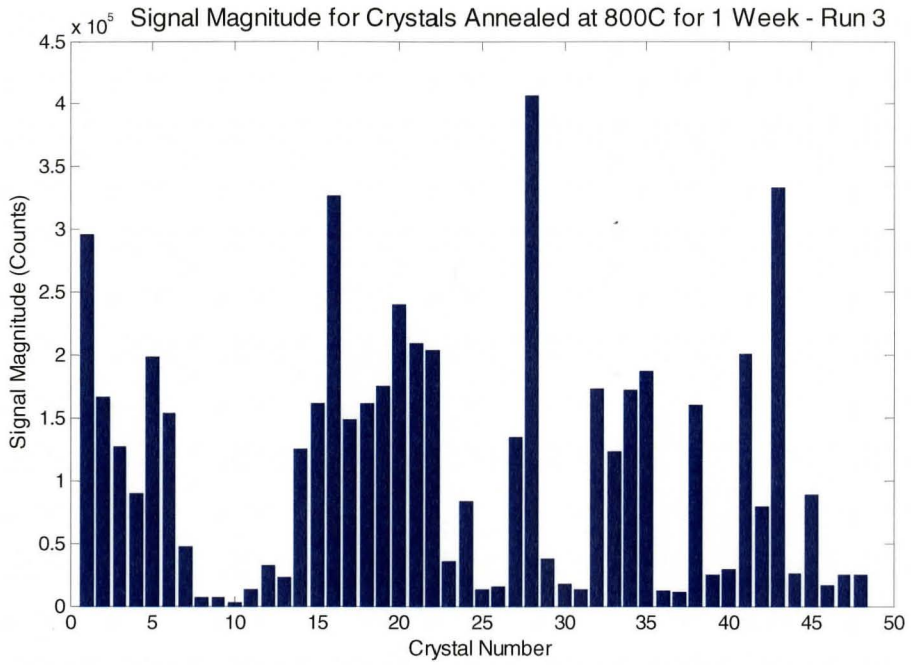

Figure 65: Average counts for 800C annealed crystals – 0.5 Gy reproduction aliquot

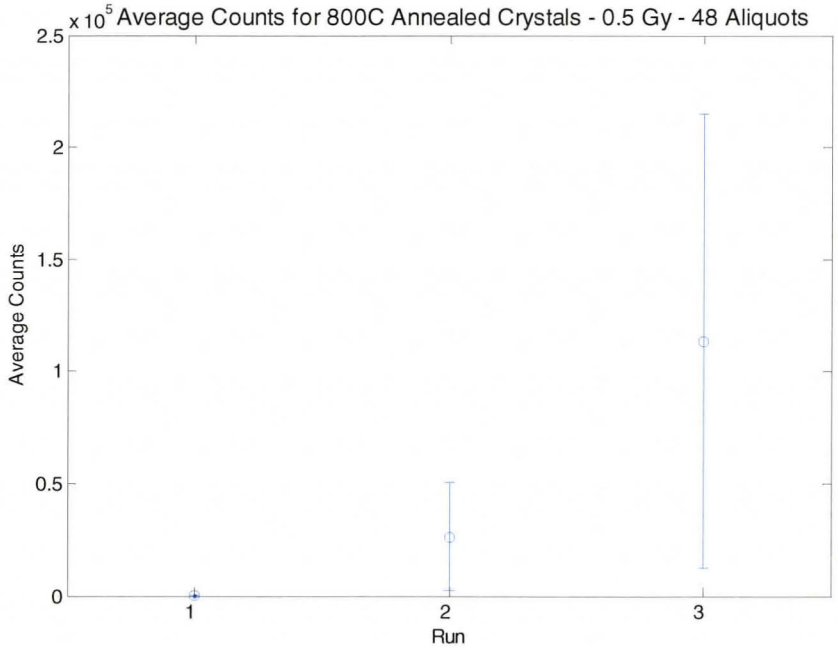

Chapter 5
Discussion

5.1 Treatment results

Untreated crystals, bleached crystals, and annealed crystals were subjected to the SAR protocol to assess which procedures result in the greatest stimulated luminescence increase for a radiation dose of 30 seconds. The bleached crystals saw a decrease in stimulated luminescence after four days of halogen light illumination, leading to the abandonment of further sensitization experiments using light exposure. Anneal treatments resulted in large gains in sensitivity and their success in improving dose estimates was investigated by lengthy annealing and cycling.

5.2 One week anneal

Thermal treatments and additional OSL runs have been shown to increase the stimulated luminescence signal from synthetic quartz and improve the dose estimates they provide. For one week anneals at 200°C, 300°C, 400°C, or 500°C the 500°C treatment increased the stimulated luminescence signal the most. In fact, the average signal magnitude for the 500°C treatment was more than double that of the next highest average signal magnitude in any other group. While it did not have the highest number of correct ED out of all treatments, the error associated with the dose estimates were smaller than for the other treatments, often in the range of 17-33% as opposed to 50-66%. This increase in sensitivity meant that all crystals treated to the 500°C anneal for one week provided ED results in both the first and second runs. In all other treatment groups some of the aliquots in the first or second run were not sufficiently sensitized as to provide a reliable signal

above background that could be fitted for ED determination. The increase in sensitivity observed at the 500°C anneal has been associated with the removal of the *E'* centre (Schilles, Poolton et al., 2001). Since the E' centre acts as a non-luminescent recombination centre, its removal increases the recombination at luminescent centers. This increased proportion of luminescent recombination increases the counts measured for a unit radiation dose, increasing the signal further above background and making dose estimation more accurate while decreasing error. The signal magnitude continued to increase after subsequent runs, suggesting that the SAR protocol was continuing to affect the crystal sensitivity.

5.3 Thermal cycling

To take advantage of this phenomenon, thermal cycling was performed to mimic the heating cycles that occur during the SAR protocol. These experiments were meant to enhance the effect that heat cycling was having upon the crystal sensitivity. Thermal cycling was performed with and without a prior 500°C one week anneal, which was shown to have the greatest sensitization enhancement tested from the previous experiment. For the crystals annealed for one week at 500°C and then subjected to 32 one hour heat cycles the greatest sensitization was recorded on the second run for the crystals cycled at 200°C, the lowest temperature used. In fact, the sensitization decreased with increasing temperature from 200°C to 500°C. This follows from the sensitization observed in the SAR protocol, which uses relatively low heats of 125°C and 160°C, but does not follow from the sensitization observed following one week annealing at 500°C. One possibility for this result is that following the one week 500°C anneal, almost all *E'*

centers have been removed from the crystals. This prevents further sensitization from occurring at elevated temperatures and so the sensitivity of these crystals remains largely unchanged after further high temperature annealing. The small difference in average signal magnitude between run 1 and run 2 at the 400°C and 500°C cycle temperatures, shown in Figure 35, supports this possibility. This explanation would also mean that there is a separate sensitization mechanism occurring at the lower temperatures used during the SAR protocol and the 200°C treatment. This low temperature sensitization mechanism is strongly supported by the 200°C data, which shows that the thermal treatment alone though annealing and cycling can increase the sensitivity of the crystals. The exact nature of this low temperature sensitization mechanism is out of the scope of this work.

Thermal cycling experiments were also carried out on crystals that did not receive a one week 500°C anneal treatment. These crystals received 32 one hour anneals at the temperatures 200°C, 300°C, 400°C, or 500°C. In this experiment the highest average signal magnitudes were from the 300°C and 400°C treatment groups. However, for all treatments and both sets of runs, no crystals had average signal magnitudes above 800 counts, far less than the near 1500 average signal counts for the one week anneals and 200°C cycle experiment. This suggests that the annealing out of the E' centre around 500°C is necessary before the low temperature sensitization mechanism works. This is supported by the 200°C treatment data in Figure 27 and Figure 28, where the second run provided an average dose signal magnitude lower than the first run.

5.4 800°C annealing

While previous long term annealing experiments and cycling experiments managed to increase sensitivity of quartz significantly, often a number of the crystals would not provide a signal above background significant enough for ED determination. To have every crystal become a functional dosimeter after treatment they were subjected to annealing at 800°C, which is known to cause the greatest increase in sensitivity in quartz (Bøtter-Jensen, Larsen et al., 1995). For the 30 second dose recovery the signal magnitude of the first run was not a major improvement over previous work; however, the second and third runs saw increases in signal magnitude of three orders of magnitude. This resulted in signals with millions of counts, as opposed to the hundreds or thousands of counts previously obtained. Further, every crystal was sensitive enough to provide an ED. This increase in sensitivity also reduced the error of the estimated doses. Regarding the ED themselves, the first run saw large underestimation of the delivered dose; this was caused by the rapidly increasing sensitivity of the crystals between the delivered dose and the test dose. This sensitivity change continued for the second run, although not as strongly. This resulted in better ED results in later runs than for the first run.

The improvement in sensitivity caused by the 800°C annealing enabled lower doses to be recovered. A smaller recovered dose of 6 seconds, representing 0.5 Gy, was used to determine if these crystals were sensitive enough to be useful as emergency dosimeters. Unlike the 2.5 Gy regeneration observed for the 800°C treated crystals, the 0.5 Gy dose did not suffer from major underestimation of the ED during the first run. In fact, for the first and second runs the ED were quite close to the correct value of 6

seconds, with estimates scattered on, slightly above, and below 6 seconds. However, for the third run, there was a tendency to overestimate the ED. This may be caused by the slowing of sensitization of the crystals with further cycling. Meaning that during the third run sensitivity change for the earlier doses in the SAR protocol was greater than the sensitivity change for the later doses. This would result in a tendency to overestimate the delivered dose and produce the observed effect of ED overestimation.

To reproduce the results observed for the 0.5 Gy recovered dose a larger group of crystals were treated to a 800°C anneal for one week. The number of crystals treated was doubled to 48; all other aspects of the protocol remained the same. For this larger group the signal magnitude results followed the same trend observed for the previous 800°C annealed crystals, where the first run saw low counts, and the second and third runs had an increase in signal by many orders of magnitude. The ED results for the first two runs were also very similar. That is, the ED were spread slightly around and on the correct value of 6. However, for the third and final run, the overestimation of dose previously observed in the group of 24 crystals was not present. The third run had ED values which fell evenly above and below the correct value without a marked skew towards underestimation or overestimation.

Chapter 6
Conclusion

The treatments outlined in this thesis enable doses of 0.5 Gy delivered to a watch crystal to be recovered within an uncertainty of 10%. However, there will need to be further research to make OSL measurement of synthetic quartz into an accurate emergency dosimeter. Three areas in particular will require additional attention. Firstly, additional information is required to ensure that treated watch crystals can act as both oscillators and dosimeters. The necessary sensitivity of synthetic quartz to resolve 0.5 Gy doses has been achieved, but the 800°C anneal treatment for 1 week may affect the oscillatory properties of the crystal since quartz at this temperature would be in the β phase and revert to α quartz upon cooling. Upon cooling to room temperature the quartz would revert back to the α phase, but this merits direct observation and the proper oscillatory frequency after treatment should be confirmed. There also needs to be confirmation that sensitized quartz undergoing oscillation in a timekeeping device would trap electrons energized to the conduction band by radiation. The vibration of the crystal lattice during oscillation may interfere with the trapping of electrons at defect sites necessary for OSL dosimetry. Secondly, timekeeping devices come in a great number of shapes and composition of materials. For example, the oscillatory component of a gamma irradiated gold watch will not record as much dose as a plastic watch subjected to the same radiation field. This is because the gold casing will absorb a greater proportion of the incident radiation than the plastic casing. Thus, though the people who had the watches may have been exposed to the same dose, the ED result from OSL measurement will suggest a smaller dose to the individual with the gold watch. This problem could be solved using a shielding factor for

the materials likely to be encountered surrounding a timekeeping device. Many materials and metals have a known shielding factor in regards to gamma radiation, which could be used to correct for the absorption caused by the casing materials. Lastly, there will necessarily be some assumptions on using an ED obtained from synthetic quartz as the delivered total body dose. In reality a person exposed to radiation may be in a building or a vehicle that will shield some of the incident radiation to varying degrees for different parts of their bodies. For example a person in a car, exposed from radiation incident from the front of the vehicle will have a higher dose delivered to their head and upper torso through the windshield, while the engine block will shield a large portion of the radiation incident to their abdomen and legs. The location of their watch during irradiation may then have a strong influence on the ED obtained and a mean to account for this should be considered for the emergency scenario

The use of synthetic quartz has much broader appeal than just wristwatches. Appendix A lists some common objects that contain synthetic quartz, and which may be used as emergency dosimeters if treated with the sensitization protocol outline above. Clearly the broad sensitization of synthetic quartz would result in having emergency dosimeters freely available in almost all environments, enabling dose reconstruction and risk assessment to proceed more accurately and mitigating some of the risks caused by nuclear technology.

Summary of conclusions

- A one week anneal at 800°C followed by two SAR protocols results in quartz crystals that can reliably recover doses as low as 0.5 Gy to a maximum of 10% error.
- Rapid increase in sensitization is likely due to annealing out of the E' centre
- Heat, irradiation, and stimulation cycling continues to improve dosimetric properties. May be due to "filling" of deep traps and non-luminescent recombination centres

Appendix A

Common objects containing synthetic quartz oscillators:

Wristwatches

Cellular Phones

Computers

Televisions

DVD Players

Microwaves

Coffee Makers

Vehicles

Clocks

Alarm Clocks

MP3 Players

Cameras

Videogame Consoles

Sprinkler systems

Bibliography

Aitken, M. J. (1998). An introduction to optical dating. New York, Oxford University Press.

Banerjee, D. (2001). "Supralinearity and sensitivity changes in optically stimulated luminescence of annealed quartz." Radiation Measurements ***33***: 47-57.

Bøtter-Jensen, L., E. Bulur, G. A. T. Duller and A. S. Murray (2000). "Advances in luminescence instrument systems." Radiation Measurements ***32***: 523-528.

Bøtter-Jensen, L., H. Jungner and V. Mejdahl (1993). "Recent developments of OSL techniques for dating quartz and feldspars." Radiation Protection Dosimety ***47***(1/4): 643-648.

Bøtter-Jensen, L., N. A. Larsen, V. Mejdahl, N. R. J. Poolton, M. F. Morris and S. W. S. McKeever (1995). "Luminescence sensitivity changes in quartz as a result of annealing." Radiation Measurements ***24***(4): 535-541.

Chang, R. (1998). Chemistry, McGraw Hill.

Chithambo, M. L. (2004). "Time-resolved luminescence from annealed synthetic quartz under 525nm pulsed green light stimulation." Radiation Measurements ***38***: 553-555.

Energy Sciences and Technology Department, B. N. L. (2008). National Nuclear Data Centre, Office of Nuclear Physics, Office of Science, U.S. Department of Energy.

Hashimoto, T., S. Sakaue, H. Aoki and M. Ichino (1994). "Dependence of TL-property changes of natural quartzes on aluminum contents accompanied by thermal annealing treatment." Radiation Measurements ***23***(2/3): 293-299.

Huntley, D. J., D. I. Godfrey-Smith and M. L. W. Thewalt (1985). "Optical dating of sediments." Nature ***313***: 105-107.

Ikeya, M. (1993). New applications of electron spin resonance. Dating, dosimetry, and microscopy, World Scientific.

Jungner, H. and L. Bøtter-Jensen (1994). "Study of sensitivity change of OSL signals from quartz and feldspars as a function of preheat temperature." Radiation Measurements ***23***(2/3): 621-624.

Kalchgruber, R., H. Y. Göksu, E. Hochhäuser and G. A. Wagner (2002). "Monitoring environmental dose rate using Risø TL/OSL readers with built-in sources: recommendations for users." Radiation Measurements ***35***: 585-590.

Kale, Y. D. and Y. H. Gandhi (2008). "Influence of pre-measurement thermal treatment on OSL of synthetic quartz measured at room temperature." Journal of Luminescence ***128***: 499-503.

Khan, R. F., D. R. Boreham and W. J. Rink (2003). "Quantification of low dose signal in EPR tooth dosimetry--a novel approach." Radiation Protection Dosimety ***103***(4): 359-362.

King, J. C. and D. B. Fraser (1961). "Performance of quartz resonators near the alpha-beta inversion point." 15th Annual Symposium on Frequency Control: 2-21.

Knoll, G. F. (2000). Radiation detection and measurement. New York, John Wiley & Sons.

Liberda, J. J., K. Schnarr, P. Coulibaly and D. R. Boreham (2005). "Artificial neural network modeling of apoptosis in gamma irradiated human lymphocytes." International Journal of Radiation Biology ***81***(11): 827-840.

Murray, A. S. and R. G. Roberts (1998). "Meaurement of the equivalent dose in quartz using a regenerative-dose single-aliquot protocol." Radiation Measurements ***29***(5): 503-515.

Murray, A. S. and A. G. Wintle (2000). "Luminescence dating of quartz using an improved single-aliquot regenerative-dose protocol." Radiation Measurements ***32***: 57-73.

Nakagawa, T. and T. Hashimoto (2003). "Sensitivity change of OSL and RTL signal from natural RTL quartz with annealing treatment." Radiation Measurements ***37***: 397-400.

Pacchioni, G., G. Ieranò and A. M. Márquez (1998). "Optical absorption and nonradiative decay mechanism of $\equiv Si^{\bullet}$ centre in Silica." Physical Review Letters ***81***(2): 377-380.

Poolton, N. R. J., G. M. Smith, P. C. Riedi, E. Bulur, L. Bøtter-Jensen, A. S. Murray and M. Adrian (2000). "Luminescence sensitivity changes in natural quartz induced by high temperature annealing: a high frequency EPR and OSL study." Journal of Physics D: Applied Physics ***33***: 1007-1017.

Schilles, T., N. R. J. Poolton, E. Bulur, L. Bøtter-Jensen, A. S. Murray, G. M. Smith, P. C. Riedi and G. A. Wagner (2001). "A multi-spectroscopic study of luminescence sensitivity changes in natural quartz induced by high-temperature annealing." Journal of Physics D: Applied Physics ***34***: 722-731.

Singarayer, J. S., R. M. Bailey and E. J. Rhodes (2000). "Potential of the slow component of quartz OSL for age determination of sedimentary samples." Radiation Measurements ***32***: 873-880.

Thomsen, K. J. (2004). Optically Stimulated Luminescence Techniques in Retrospective Dosimetry using Single Grains of Quartz extracted from Unheated Materials, University of Copenhagen, Denmark. ***Ph.D.:*** 176.

Veronese, I., V. Schved, E. A. Shishkina, A. Giussani and H. Y. Göksu (2007). "Study of dose rate profile at sample disks in a Risø OSL single-grain attachment system." Radiation Measurements ***42***: 138-143.

Zimmerman, J. (1971). "The radiation-induced increase of the 100C thermoluminescence sensitivity of fired quartz." Journal of Physics C: Solid State Physics ***4***: 3265-3276.